



**International Masters of Science in Environmental Technology and Engineering**

Master's dissertation submitted in partial fulfilment of the requirements for the joint degree of  
EU Erasmus+ Master course organized by  
University of Chemistry and Technology, Prague, the Czech Republic  
IHE Delft Institute for Water Education, Delft, the Netherlands  
Ghent University, Ghent, Belgium

Academic year 2023-2024

# Methanotroph-microalgae carbon neutral process for the production of ectoine from biogas

Centre for Microbial Ecology and Technology (CMET)

Patricia Mohedano Caballero

Promotor: Jo De Vrieze

Co-promotor: Patricia Ruiz Ruiz





**International Masters of Science in Environmental Technology and Engineering**

Master's dissertation submitted in partial fulfilment of the requirements for the joint degree of  
EU Erasmus+ Master course organized by  
University of Chemistry and Technology, Prague, the Czech Republic  
IHE Delft Institute for Water Education, Delft, the Netherlands  
Ghent University, Ghent, Belgium

Academic year 2023-2024

# Methanotroph-microalgae carbon neutral process for the production of ectoine from biogas

Centre for Microbial Ecology and Technology (CMET)

Patricia Mohedano Caballero

Promotor: Jo De Vrieze

Co-promotor: Patricia Ruiz Ruiz



This is an unpublished M.Sc. dissertation and is not prepared for further distribution. The author and the promoter give the permission to use this Master dissertation for consultation and to copy parts of it for personal use. Every other use is subject to the copyright laws, more specifically the source must be extensively specified when using results from this Master dissertation.

## **ACKNOWLEDGEMENTS**

I wish to particularly acknowledge my co-promotor, Dr. Eng. Patricia Ruiz Ruiz, and my promotor, Prof. Dr. Jo de Vrieze, for their invaluable contributions to the development of my thesis. Without their support, this thesis would not have reached its current level of quality. This research journey has been a substantial learning experience for me, and I have evolved as a scientist thanks to their guidance. Patricia has been an outstanding mentor, from whom I acquired an immense amount of knowledge as well as relevant practical experience. She was always willing to assist me anytime selflessly and always encouraged me to perform at my best. I would also like to extend my sincere gratitude to all CMET members who made my time at the lab more enjoyable and were always there to assist me with any inquiries I had.

I am deeply grateful to all my classmates of IMETE program with whom I have created a lot of unforgettable memories and gained valuable life lessons over the past two years. I thank the European commission for providing me this life-changing opportunity through a programme country scholarship to pursue the Erasmus Mundus IMETE program (2017-1957/001-001-EMJMD) in UCT Prague, IHE Delft Institute for Water Education and Ghent University. I am extremely grateful for the opportunities it has given me and the relationships I have built along the way.

Last but not least, I thank my beloved family for their unconditional support throughout this journey, no matter the distance or wherever life takes me. They have always given me the chance to pursue my dreams and for that, I am forever grateful. This thesis is dedicated to them with all my love.

## ABSTRACT

Human activities and industrial development are the main drivers of global climate change, leading to unprecedented levels of greenhouse gases (GHG), primarily carbon dioxide (CO<sub>2</sub>) and methane (CH<sub>4</sub>), in the atmosphere. Co-culturing methanotrophic bacteria with microalgae presents a promising approach for converting biogas — containing both CH<sub>4</sub> and CO<sub>2</sub> — into valuable ectoine-synthesising biomass by coupling CH<sub>4</sub> oxidation with oxygenic photosynthesis. Ectoine, a bacterial osmoprotectant, is widely utilized in the pharmaceutical and cosmetic industries with a significant market value (600-1,000 € kg<sup>-1</sup>). In this study, microbial communities were enriched from four environmental samples of the North Sea coast on the Belgian-Dutch border: Sediment, North Sea, River and Combination. The Sediment enrichment exhibited the highest CH<sub>4</sub> removal efficiency (87.7%) and ectoine synthesis ( $6.7 \pm 1.4 \text{ mg}_{\text{ectoine}} \text{ g}_{\text{VSS}}^{-1}$ ), primarily comprising the microalgae *Picochlorum oklahomense* and the methanotrophic and methylotrophic bacteria *Methylobacter marinus* and *Methylophaga marina*, among other heterotrophic bacteria. The optimal growth conditions and ectoine production of this culture under varying salinity levels and osmotic stress were also investigated. Salinity tests revealed that NaCl concentrations of 6% or higher negatively impacted CH<sub>4</sub> oxidation and inhibited ectoine synthesis after 14 days of incubation, while osmotic shocks highlighted the potential for ectoine accumulation, peaking at  $51.3 \text{ mg}_{\text{ectoine}} \text{ g}_{\text{VSS}}^{-1}$  under 4.5% NaCl conditions. The results demonstrate the adaptability of the enriched consortia and their potential for GHG mitigation and high-value chemicals production. This pioneering work marks an important step toward harnessing methanotroph-microalgae interactions for sustainable biogas valorisation into ectoine, aiming for a carbon-neutral process.

Keywords: Biogas, ectoine, methanotrophs, microalgae, enrichments.

# TABLE OF CONTENTS

	Page
ACKNOWLEDGEMENTS .....	i
ABSTRACT.....	ii
TABLE OF CONTENTS.....	iii
LIST OF TABLES .....	v
LIST OF FIGURES .....	vi
LIST OF SYMBOLS AND ABBREVIATIONS .....	ix
1. INTRODUCTION.....	1
1.1. Current state of biogas production and utilization.....	1
1.2. Methanotrophs.....	3
1.3. Microalgae.....	5
1.4. Methalgae .....	7
1.5. Ectoine .....	10
2. OBJECTIVES .....	14
3. MATERIALS AND METHODS .....	15
3.1. Experimental outline.....	15
3.2. Enrichments from a saline environment.....	15
3.2.1. Sampling site description .....	15
3.2.2. Culture conditions.....	16
3.3. Salinity test: Influence of NaCl concentration on growth, ectoine production and gas consumption.....	17
3.4. Osmotic shock tests .....	17
3.5. Analytical techniques .....	18
3.5.1. Gas chromatography (GC).....	18
3.5.2. Microbial growth.....	18
3.5.3. pH.....	19
3.5.4. Ectoine .....	19
3.5.5. Flow cytometry .....	19
3.6. Molecular characterization .....	20
3.7. Calculations and statistical analysis .....	20
4. RESULTS .....	22
4.1. Enrichments from saline environments .....	22
4.1.1. Gas evolution in the enrichments.....	22
4.1.2. Methane removal efficiencies .....	23
4.1.3. Microbial composition .....	23
4.1.4. Ectoine content and biomass growth.....	25

4.2.	Salinity tests: Influence of NaCl concentration on growth, ectoine production and gas consumption.....	26
4.2.1.	Methane removal efficiency and gas concentration in the headspace .....	26
4.2.2.	Biomass growth and composition .....	28
4.2.3.	Ectoine production .....	30
4.3.	Osmotic shock tests .....	30
4.3.1.	Methane removal efficiency and gas concentrations in the headspace.....	30
4.3.2.	Biomass growth and composition .....	33
4.3.3.	Ectoine production .....	34
5.	DISCUSSION .....	36
5.1.	Enrichments from saline environments .....	36
5.2.	Salinity tests: Influence of NaCl concentration on growth, ectoine production and gas consumption.....	37
5.3.	Osmotic shock tests .....	38
6.	CONCLUSIONS AND PERSPECTIVES .....	41
7.	REFERENCES.....	42
8.	APPENDIX .....	49
8.1.	Comparative analysis of economic viability of methanotrophic biomass calculations for ectoine production versus biogas combustion for energy production.....	49
8.2.	Shock tests FCM results .....	50

## LIST OF TABLES

<b>Table 1.</b> Primary risks associated with each stage of biogas production, collection, transportation and storage in decentralized biogas digesters (adapted from Marrazzo & Mazzini, 2024). .....	1
<b>Table 2.</b> Existing studies of the methanotroph-photoautotroph cooperative systems. ....	8
<b>Table 3.</b> Previous studies on ectoine production from biogas by methanotrophic or microalgae systems. ....	12
<b>Table 4.</b> Site characteristics and sample initial characterization.....	16
<b>Table 5.</b> Mineral salts medium composition without additional NaCl. ....	17
<b>Table 6.</b> Percentage of NaCl over the experimental time in the three osmotic shock tests conducted: OS1, OS2 and OS3. ....	18
<b>Table 7.</b> Main characteristics of prokaryotic and eukaryotic organisms related to the sequences retrieved from Sediment enriched sample.....	24
<b>Table 8.</b> Specific ectoine values in current methanotroph studies .....	39
<b>Table 9.</b> Microbial composition of the shock tests experimental groups OS1, OS2, OS3 obtained from FCM analysis. ....	50



## LIST OF FIGURES

<b>Figure 1.</b> Diverse methane oxidation pathways of different groups of methanotrophs (Kalyuzhnaya et al., 2015). .....	4
<b>Figure 2.</b> Bioproducts potential to be obtained by methanotrophs and their schematic metabolic pathways (Jawaharraj et al., 2020; Kalyuzhnaya et al., 2015). .....	5
<b>Figure 3.</b> Photosynthesis mechanism scheme of its biochemical and biophysical processes (Yang et al., 2020). .....	6
<b>Figure 4.</b> Methalgae scheme of the interaction of methanotrophs and microalgae and possible bioproducts of synthesis (adapted from Ruiz-Ruiz et al., 2020). .....	7
<b>Figure 5.</b> Chemical structure of ectoine (A) and hydroxyectoine (B) (Tanne et al., 2014). .....	10
<b>Figure 6.</b> Schematic overview of the EctoMet project and its Work Packages (WP). Green microorganisms depict microalgae, red methanotrophs, blue and yellow satellite species. ....	14
<b>Figure 7.</b> Overview of the experimental work performed during this master thesis. 1) Selection of the methalgae enrichment that presented the highest CH <sub>4</sub> removal efficiencies, 2) determination of most suitable NaCl concentration for the methalgae growth and 3) evaluation of the culture performance under different osmotic shock stress conditions.....	15
<b>Figure 8.</b> Site, sampling points and samples.....	16
<b>Figure 9.</b> Intracellular ectoine extraction and measurement protocol. ....	19
<b>Figure 10.</b> Amount of methane (CH <sub>4</sub> ), oxygen (O <sub>2</sub> ) and carbon dioxide (CO <sub>2</sub> ) in milligrams (mg) in the headspace of the serum bottles during the enrichment period for the four different North Sea samples shown as: A) Sediment (10 weeks incubation). B) River (6 weeks incubation). C) North Sea (4 weeks incubation). D) Combination (8 weeks incubation). .....	22
<b>Figure 11.</b> Average CH <sub>4</sub> removal efficiency per 2-day replenishment for each enrichment during the entire incubation period. The error bars indicate the standard deviation of each value. ....	23
<b>Figure 12.</b> Relative abundance of the prokaryotic and eukaryotic amplicon sequencing variants (ASV) found in the Sediment enrichment. A) Prokaryotes. B) Eukaryotes.....	24
<b>Figure 13.</b> Light microscopy image (20x) of the Sediment enrichment showcasing a mixed culture of <i>Picochlorum oklahomense</i> and different bacteria.....	25
<b>Figure 14.</b> Average CH <sub>4</sub> removal efficiency per 2-day replenishment for each NaCl concentration test (0%, 3%, 6% and 9% NaCl). The error bars indicate the standard deviation of biological duplicates. .	26
<b>Figure 15.</b> Amount of methane (CH <sub>4</sub> ), oxygen (O <sub>2</sub> ) and carbon dioxide (CO <sub>2</sub> ) in milligrams (mg) in the headspace of the experimental groups 0%, 3%, 6% and 9% NaCl during the 14-day experimental period, with headspace replenishment every 2 days, shown as follows: 0A) 0% NaCl biological duplicate 0B) 0% NaCl biological duplicate B. 3A) 3% NaCl biological duplicate A that suffered	

photoinhibition in the fourth day of incubation 3B) 3% NaCl biological duplicate B. 6A) 6% NaCl biological duplicate 6B) 6% NaCl biological duplicate B. 9A) 9% NaCl biological duplicate A that suffered photoinhibition in the fourth day of incubation. 9B) 9% NaCl biological duplicate B. .... 27

**Figure 16.** Salinity test biological duplicates for NaCl concentrations of 0%, 3%, 6% and 9% at two points: A) start of the experiment and B) after 14-day incubation period. Photoinhibition clearly visible in duplicates 3A and 9A from fourth day onwards and upon completion of the experiment. .... 28

**Figure 17.** Average biomass concentration in  $g_{VSS} L_{culture}^{-1}$  of the initial inoculum and final measurement of biological duplicates for each salinity concentration test (0%, 3%, 6% and 9%). The error bars indicate the standard deviation of test. .... 29

**Figure 18.** Relative abundance (in percentage) of microalgae and heterotrophic/methanotrophic bacteria in the initial inoculum and each salinity test (for both biological duplicates A and B) after 14 days of culture. .... 29

**Figure 19.** Example of FCM results obtained from the 3% experiment, along with the gating performed for microalgae-bacteria determination. A). Filtered mineral salt medium with 3% NaCl. B) 3%A photoinhibited bioreactor. C) 3%B non-photoinhibited bioreactor. .... 29

**Figure 20.** Average intracellular ectoine concentration in  $mg_{\text{ectoine}} g_{VSS}^{-1}$  initially (initial inoculum) and after 14 days of incubation for both biological duplicates at 0%, 3%, 6% and 9% NaCl. The error bars indicate the standard deviation of biological duplicates. .... 30

**Figure 21.** Average CH<sub>4</sub> removal efficiencies (and standard deviation in the form of error bars) from biological duplicates with different NaCl concentrations in each replenishment and denoted as OS1, OS2 and OS3 per 1-day replenishment. +: Mineral salt medium with 4.5% NaCl osmotic shock. ++: Mineral salt medium with 6% NaCl osmotic shock. The error bars indicate the standard deviation of each value. .... 31

**Figure 22.** Amount of methane (CH<sub>4</sub>), oxygen (O<sub>2</sub>) and carbon dioxide (CO<sub>2</sub>) in milligrams (mg) in the headspace of the experimental groups OS1, OS2 and OS3 during the 5-day osmotic shock tests shown as follows: OS1A. Osmotic shock tests biological duplicate A with first shock (\*) at 4.5% NaCl concentration and second shock at 6% NaCl concentration (\*\*). OS1B. Osmotic shock tests biological duplicate B with first shock (\*) at 4.5% NaCl concentration and second shock at 6% NaCl concentration (\*\*). OS2A. Osmotic shock tests biological duplicate A with first (\*) and second shock (\*\*) at 4.5% NaCl concentration. OS2B. Osmotic shock tests biological duplicate B with first (\*) and second shock (\*\*) at 4.5% NaCl concentration. OS3A. Osmotic shock tests biological duplicate A with first (\*) and second shock (\*\*) at 6% NaCl concentration. OS3B. Osmotic shock tests biological duplicate B with first (\*) and second shock (\*\*) at 6% NaCl concentration. All cultures were maintained in a 3% NaCl concentration medium during days 1 to 2 and 4 to 5 of the experiment. .... 32

**Figure 23.** Average biomass growth in  $g_{vss} L^{-1}$  per 1-day replenishment for the biological duplicates of each osmotic shock test. OS1) initially grown in a mineral salt medium (MSM) containing 3% NaCl followed by a first osmotic shock with raised NaCl concentration (4.5%), a second osmotic shock 6% NaCl content and a final culture back at 3% NaCl content. OS2) initially grown in a MSM containing 3% NaCl followed by a first and second osmotic shocks with raised NaCl concentration (4.5%) and a final culture back at 3% NaCl content. OS3) initially grown in a MSM containing 3% NaCl followed by a first and second osmotic shocks with raised NaCl concentration (6%) and a final culture back at 3% NaCl content. The error bars indicate the standard deviation of each value. .... 33

**Figure 24.** Osmotic shock test biological duplicates after 7-day incubation period. .... 34

**Figure 25.** Intracellular ectoine concentration measured before the osmotic shock experiments, after first and second shocks, and upon returning to 3% NaCl for the three experimental osmotic shock test groups: OS1, OS2 and OS2. The OS1 experimental group was initially subjected to a 4.5% NaCl shock (first shock: \*) followed by a 6% NaCl osmotic shock (second shock: \*\*). The OS2 group was exposed to a 4.5% NaCl osmotic shock on both days (first and second shock: \* and \*\*), while the OS3 group underwent a 6% NaCl shock on both days (first and second shock: \* and \*\*). .... 35

## LIST OF SYMBOLS AND ABBREVIATIONS

AD	Anaerobic digestion
ASV	Amplicon sequencing variants
ATP	Adenosine triphosphate
bcm	Billion cubic meters
C	Combination sample
CH <sub>4</sub>	Methane
CH <sub>4</sub> RE	Methane removal efficiency
CO <sub>2</sub>	Carbon dioxide
CO <sub>2</sub> -eq	Carbon dioxide equivalent
EU	European Union
FCM	Flow cytometry
GHG	Atmospheric greenhouse gases
GWP	Global warming potential
h	hours
H <sub>2</sub> S	Hydrogen sulphide
HPLC-UV	High-performance liquid chromatography with ultra-violet spectroscopy
m <sup>3</sup>	Cubic metre
min	Minutes
MOB	Methane oxidizing bacteria
µm	Micrometre
N	Nitrogen
NaCl	Sodium chloride
NADPH	Nicotinamide adenine dinucleotide phosphate
NO <sub>3</sub> <sup>-</sup>	Nitrate
NS	North Sea sample
O <sub>2</sub>	Oxygen
PM	Particulate matter
PHAs	Polyhydroxyalkanoates
PHBs	Polyhydroxybutyrates
pMMO	Particulate enzyme methane monooxygenase
PSI	Photosystem I
PSII	Photosystem II
R	River sample
RuBisCO	Ribulose-1,5-bisphosphate carboxylase oxygenase
RuMP	Ribulose monophosphate pathway
S	Sediment sample
SCP	Single cell protein
sMMO	Soluble enzyme methane monooxygenase
TN	Total nitrogen
TP	Total phosphorus
TSS	Total suspended solids
VOCs	Volatile organic compounds
VSS	Volatile suspended solids
WWTPs	Wastewater treatment plants

# 1. INTRODUCTION

## 1.1. Current state of biogas production and utilization

Human activities and industrialization are the main drivers of global climate change, with atmospheric greenhouse gas (GHG) concentrations reaching unprecedented levels. Carbon dioxide (CO<sub>2</sub>) is the most significant contributor, accounting for 77% of total emissions, while methane (CH<sub>4</sub>) contributes a 15% and has a global warming potential (GWP) between 20 to 34 times greater than CO<sub>2</sub> (IPCC, 2023). The rise in GHG levels, with global gas emissions in 2021 reaching 34.9 gigatons of carbon dioxide equivalents (Gt CO<sub>2</sub>-eq), has led to a 0.87°C increase in global temperatures, with projections indicating further increases of 1-3.7°C in the coming decades. Hence, efforts to reduce CH<sub>4</sub> and CO<sub>2</sub> emissions are crucial to limit global warming to 1.5°C above preindustrial levels by 2030 (IPCC, 2018).

Anaerobic processes, such as anaerobic digestion (AD), produce CH<sub>4</sub> and CO<sub>2</sub> from the anaerobic decomposition of organic matter in anaerobic environments, such as landfills, rice paddies, and the digestive tracts of ruminant animals (Geşicka et al., 2024). These gases are also released during the extraction and transportation of fossil fuels, organic waste disposal, wastewater treatment, and bioenergy production in the form of diffusive emissions (Wang et al., 2022). In controlled AD processes the main purpose is to produce biogas maximizing CH<sub>4</sub> production for power and heat generation. In contrast, diffusive emissions refer to unintended CH<sub>4</sub> and CO<sub>2</sub> emissions whose release into the atmosphere should be minimized or avoided to reduce the greenhouse gas footprint and protect the environment (Gómez-Borraz et al., 2017).

Biogas consists mainly of CH<sub>4</sub> (50–70%) and CO<sub>2</sub> (30–50%), and usually needs to be upgraded or cleaned for its use in heat, power, and transportation applications. Biogas production is generally considered a positive approach for sustainable energy recovery, but the risks in its production, collection, storage, and transportation affect the operational stability of biogas production facilities, especially decentralized biogas digesters (Table 1). Decentralized small-scale biogas digesters tend to have unstable sources of AD feedstock leading to low CH<sub>4</sub> concentration, which makes the conversion from biogas into energy/heat recovered, range only from 20 to 40%. This makes uneconomically feasible to use biogas produced in a decentralized manner for power/heat generation, resulting in the flaring of this gas, or in the worst case-scenario, venting. These practices not only significantly contribute to CH<sub>4</sub> and CO<sub>2</sub> emissions but also represent a substantial waste of energy, missing out on a valuable economic opportunity due to the biogas' potential (Li et al., 2022).

**Table 1.** Primary risks associated with each stage of biogas production, collection, transportation and storage in decentralized biogas digesters (adapted from Marrazzo & Mazzini, 2024).

<b>Production</b>	<b>→</b>	<b>Collection</b>	<b>→</b>	<b>Transportation</b>	<b>→</b>	<b>Storage</b>
<i>Feedstock quality:</i> feedstock composition can impact biogas quality and composition by increasing its impurities (like hydrogen sulphide, H <sub>2</sub> S) which can be fatal for living organisms or deteriorate the equipment.		<i>Explosion risk:</i> CH <sub>4</sub> is highly flammable and can lead to explosions at concentrations higher than 10% in presence of oxygen (O <sub>2</sub> ).		<i>Leakage:</i> can lead to explosive atmospheres and environmental hazards.		<i>Explosion and fire hazard:</i> biogas storage in high-pressure tanks can poses a significant risk of explosion if not managed correctly.

---

<p><i>Biogas composition:</i> if CH<sub>4</sub> levels do not reach a minimum percentage, its collection is not economically feasible leading to gas flaring which emits air pollutants like particulate matter (PM), volatile organic compounds (VOCs) and sulphur dioxide (SO<sub>2</sub>). Also, it is an explosive hazard if there is biogas accumulation promoting GHG emissions.</p>	<p><i>O<sub>2</sub> displacement:</i> biogas can displace O<sub>2</sub> by being heavier than air leading to asphyxiation risks in confined spaces.</p>	<p><i>Pressure management:</i> improper management of biogas pressure can lead to bursts or leaks.</p>	<p><i>O<sub>2</sub> displacement:</i> biogas can displace O<sub>2</sub> by being heavier than air leading to asphyxiation risks in confined spaces.</p>
--	---	--	---

---

The utilization of biogas as a renewable energy source has gained significant attention in recent years, as countries strive to reduce their reliance on fossil fuels and combat climate change. In late 2019, the European Commission made a bold pledge to reach zero net greenhouse gas emissions by 2050. This commitment, known as the European Green Deal (COM/2019/640 final), requires the participation of all international partners to develop and optimize processes to prevent "carbon leakage" (De Vrieze, 2020). In this context, biomethane production, which involves upgrading biogas to a higher purity level, has emerged as a key focus area for the European Union (EU) and its member states (European Commission: Energy, Climate Change, Environment, 2022). As part of the EU's broader efforts to increase the supply of bioenergy, biomethane has become a key contributor to renewable energy consumption, with biogas/biomethane accounting for 10.1% of bioenergy production – or 20.2 bcm (billion cubic meters) – in the EU in 2021. By 2030, the EU has set ambitious targets for biomethane generation aiming to achieve 35 bcm annually, with an estimated investment need of €37 billion (European Commission: Energy, Climate Change, Environment, 2023).

The need to scale-up biomethane production is underscored by the EU's REPowerEU Plan, launched in response to the energy market disruptions caused by Russia's invasion of Ukraine in 2022. The plan aims to reduce the EU's dependence on Russian fossil fuel imports by increasing energy efficiency, diversifying energy supplies, and ramping up renewable energy production. As part of this plan, the EU is working to accelerate investments in biomethane production and create an industrial partnership to support the growth of sustainable biomethane use. With a 30% stable annual growth rate in biomethane production capacity, this target can be achieved (European Commission: Energy, Climate Change, Environment, 2022).

In Belgium, biomethane production has shown promising growth, with energy balances from 2021 recording 0.3 bcm of biogas produced, accounting for 1.6% of the country's gas supply. However, the potential for biomethane production in Belgium remains largely untapped, with industry estimates suggesting a potential of 0.6 bcm by 2030. As of 2021, Belgium has a total of 40 medium and large-scale anaerobic digestion plants and 109 small-scale plants (with 29 located in the Wallonia region and 80 in Flanders) (European Biogas Association, 2021). Belgium has developed a robust system of anaerobic digesters at small, medium and large scales to treat food waste, crops, livestock manure, and agricultural residues, producing biogas as second-generation form of bioenergy. Therefore, Belgium's biomethane market holds significant potential for reducing greenhouse gas emissions, promoting the achievement of "carbon neutrality", and enhancing energy security through the displacement of natural gas imports (Li et al., 2022). However, due to the rapid advancement of the Belgian biogas sector, there

is an urgent need for alternative strategies for biogas utilization, especially when energy production from biogas is not feasible (European Biogas Association, 2021).

Converting biogas into higher-value products becomes essential to justify investments in biogas capture and utilization. Biological technologies offer a cost-effective and environmentally friendly approach to biogas valorisation, or GHG emission mitigation, compared to traditional physical and chemical methods. This is because they usually involve simpler processes that operate at ambient temperature and pressure, making them a more sustainable option (Ruiz-Ruiz et al., 2020; Ruiz-Ruiz et al., 2024). Through biological processes, photosynthetic organisms, including microalgae, can capture and utilize CO<sub>2</sub>, while methane oxidizing bacteria (MOB) oxidize CH<sub>4</sub>, contributing to managing atmospheric carbon levels and offering potential applications across various industries.

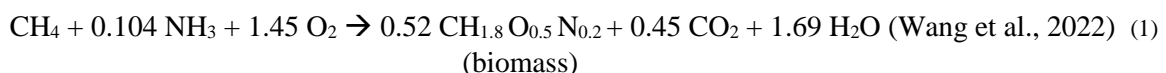
The biological conversion of CH<sub>4</sub> to higher-value products by methanotrophic organisms has emerged as a promising solution to address CH<sub>4</sub> emissions and unlock the potential value of CH<sub>4</sub> as a carbon source (Strong et al., 2016). Microalgae do also have high potential to address CO<sub>2</sub> emissions and produce a wide variety of metabolites with industrial interest such as proteins, lipids, carbohydrates and pigments (González-González & De-Bashan, 2021). By harnessing biological processes, CH<sub>4</sub> and CO<sub>2</sub> conversion technologies offer a sustainable and economically viable pathway to reduce their emissions and contribute to the transition towards a low-carbon future (Ruiz-Ruiz et al., 2024).

However, several are the technical challenges associated with the valorisation of biogas: its only carbon source is in a gas form meaning it has mass transfer limitations, impurities in the biogas (e.g. H<sub>2</sub>S), oxygen limitation, and CO<sub>2</sub> accumulation, make it have lower biomass growth rates in comparison to other carbon sources. Potential solutions for enabling the use of biogas as a carbon substrate are enhance solubility in the culturing parameters, have a tight control on the biogas fed and mainly the use of methanotroph-microalgae co-cultures to ensure an efficient CH<sub>4</sub> oxidation with lower CO<sub>2</sub> emissions and less limited O<sub>2</sub> supply (Jawaharraj et al., 2020).

## 1.2. Methanotrophs

Methanotrophs are part of a larger group called methylotrophs, a diverse group of bacteria known for their ability to utilize single-carbon compounds, such as methane, methanol, formic acid, and formaldehyde as carbon and energy sources (Hanson & Hanson, 1996). Methanotrophs only assimilate CH<sub>4</sub> as their sole carbon and energy source and play a crucial role in the global carbon cycle. Most reported methanotrophs are aerobic, oxidizing CH<sub>4</sub> into CO<sub>2</sub>, a process that requires molecular O<sub>2</sub>. These bacteria are commonly found in a wide range of habitats, including activated sludge, landfills, marine sediments, rice fields, and other environments associated with CH<sub>4</sub> emissions (Safitri et al., 2021; Geçsicka et al., 2024).

From a biological perspective, aerobic methanotrophs utilize CH<sub>4</sub> as a carbon source to meet their metabolic needs, producing CO<sub>2</sub> as a by-product of their metabolism (Jawaharraj et al., 2020). This process can be described by the following equation:



Methanotrophs had been typically classified into four groups based on their carbon fixation metabolism: Type I methanotrophs (Gammaproteobacteria class, Pseudomonadota phylum), Type II (Alphaproteobacteria class, Pseudomonadota phylum), Type III (Verrucomicrobiota phylum) and Type X (Gammaproteobacteria, Pseudomonadota phylum) (Hanson & Hanson, 1996; Oren & Garrity, 2021). Type I methanotrophs assimilate methane-derived carbon through the ribulose monophosphate pathway

(RuMP), thrive in oxygen-rich environments and are known for their higher growth rates compared to Type II methanotrophs. Main genera in this type are *Methylomonas*, *Methylobacter* and *Methylococcus*. Type II methanotrophs fix carbon through the serine cycle and are more adaptable to diverse environmental conditions, including genera like *Methylosinus* and *Methylocystis*. Type X methanotrophs are also part of the Gammaproteobacteria class and use the RuMP pathway for carbon assimilation, but have some characteristics from Type II methanotrophs. The main representative of this type is *Methylococcus capsulatus*. Verrucomicrobiota methanotrophs are mixotrophic, meaning they can utilize multiple carbon sources (Gęsicka et al., 2024; Strong et al., 2016).

The first step in aerobic methane metabolism is the oxidation of methane to methanol by the enzyme methane monooxygenase (MMO), which can occur in both soluble (sMMO) and membrane-associated particulate (pMMO) forms. Methanol is further oxidized to formaldehyde, formate, and carbon dioxide, or assimilated into cellular components. Methanotrophs span different bacterial classes, including Gammaproteobacteria, Alphaproteobacteria, and Verrucomicrobiota, with different metabolic pathways for CH<sub>4</sub> oxidation and carbon assimilation, as shown in Figure 1 (Khmelenina et al., 2018; Strong et al., 2016).

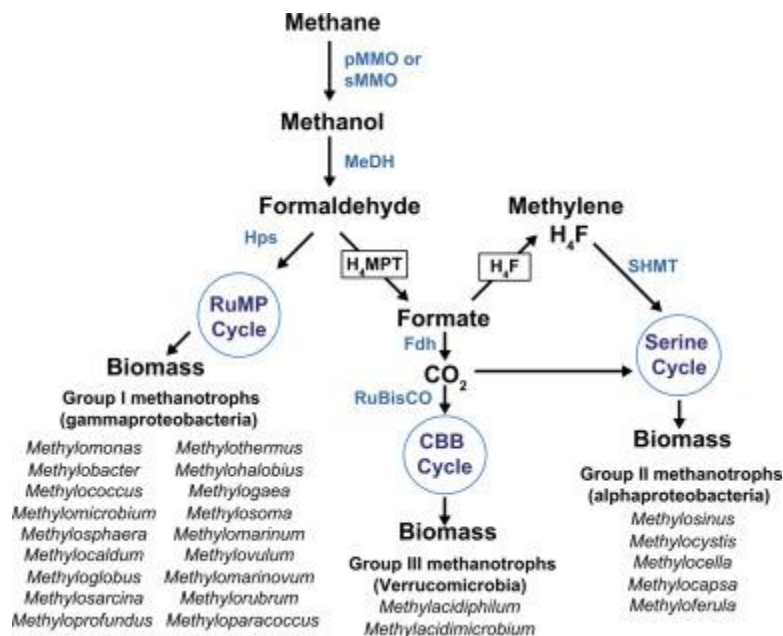


**Figure 1.** Diverse methane oxidation pathways of different groups of methanotrophs (Kalyuzhnaya et al., 2015).

Methanotrophic bacteria are metabolically versatile as they display diverse physiological requirements, with different growth conditions, O<sub>2</sub> requirements, and nutrient preferences depending on their metabolic pathways and environmental niches (Khmelenina et al., 2018). Due to their unique ability to utilize CH<sub>4</sub> as an energy and carbon source, they have significant biotechnological applications that span across diverse fields including environmental management, biomedical compound production and biofuel production (Figure 2). From an environmental standpoint, they play a crucial role in CH<sub>4</sub> mitigation by removing CH<sub>4</sub> generated by methanogens both in natural and anthropogenic sources. Additionally, they can remove nitrogen (N) compounds, like ammonia and nitrate, making them valuable in wastewater treatment plants (WWTPs). In the chemical field, methanotrophs are utilized as catalysts for fuel and chemical production mainly methanol (a valuable intermediate compound) and polyhydroxyalkanoates (PHAs) used as a bioplastic (Guerrero-Cruz et al., 2021; Lee, 2019b). Methanotroph-produced molecules like ectoine, PHAs, methanobactin, carotenoids, unsaturated fatty acids, and single cell protein (SCP), are recently under the scope due to their promising applications in



biomedicine (Salem et al., 2021). As an example, methanotrophic biomass can produce 574 mg of ectoine from one mole of biogas, resulting in 35 grams of ectoine per kilogram of biomass. This has a market value of 10 to 17 euros per cubic meter of biogas, which is considerably higher than the 2 to 3.5 euros per cubic meter of biogas obtained from biogas burning into energy conversion (Appendix 8.1). Given that the final product — microbial biomass — is significantly more valuable than electricity, it can be more preferable to convert CH<sub>4</sub> into microbial biomass rather than burning it for electricity. However, achieving cost competitiveness for methane-derived products compared to current industrial processes remains a challenge, due to low efficiency gas-to-liquid mass transfer, the complexity involved in biomass production, high costs associated with extraction and purification, and the substantial investments still required in research and development to optimize these processes (Lim et al., 2024; Roberts et al., 2020).

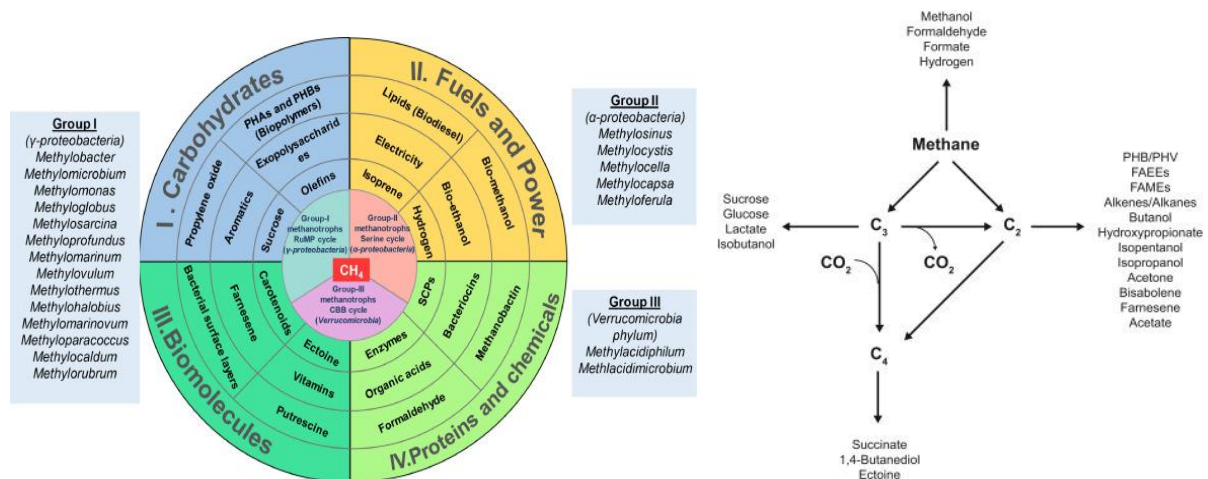


**Figure 2.** Bioproducts potential to be obtained by methanotrophs and their schematic metabolic pathways (Jawaharraj et al., 2020; Kalyuzhnaya et al., 2015).

### 1.3. Microalgae

Microalgae, a polyphyletic group of both eukaryotic and prokaryotic photosynthetic microorganisms, including Chlorophyta (green algae), Rhodophyta (red algae), Phaeophyceae (brown algae), and diatoms, play a crucial role in carbon mitigation, as they can grow much faster than terrestrial plants, have a 10-50 times higher CO<sub>2</sub> fixation efficiency, and can live in harsh conditions, due to their unicellular or simple multicellular structure (Zhang, 2018; Ruiz-Ruiz et al., 2020b).

Photosynthesis, the fundamental process by which green plants, algae, and some bacteria convert light energy into chemical energy, is essential for life on Earth. Through photosynthesis, organisms capture sunlight and use it to produce energy-rich organic molecules, like glucose, which serve as a source of fuel for metabolism and growth. Central to this process is the conversion of light energy into chemical energy, which occurs through a series of biochemical reactions in two main stages: the light reactions and the dark reactions.

The light reactions of photosynthesis take place in the thylakoid membranes of chloroplasts in plants and algae. These reactions capture light energy and convert it into chemical energy in the form of ATP (adenosine triphosphate) and reducing equivalents in the form of NADPH (nicotinamide adenine dinucleotide phosphate). The key players in the light reactions are the pigment-protein complexes Photosystem II (PSII) and Photosystem I (PSI), which absorb light and transfer energy to reaction centres where water is split to release O<sub>2</sub> and generate electrons. These electrons are then passed through a series of electron carriers to produce NADPH and ATP. In addition to the linear electron transport chain, a cyclic pathway also exists in which electrons are recycled to generate a proton gradient that

drives ATP synthesis. This cyclic pathway helps maintain the balance of ATP and NADPH required for the dark reactions of photosynthesis, where carbon dioxide is fixed and converted into carbohydrates via the Calvin-Benson cycle (Figure 3) (Ruiz-Ruiz et al., 2020b; Jawaharraj et al., 2020).

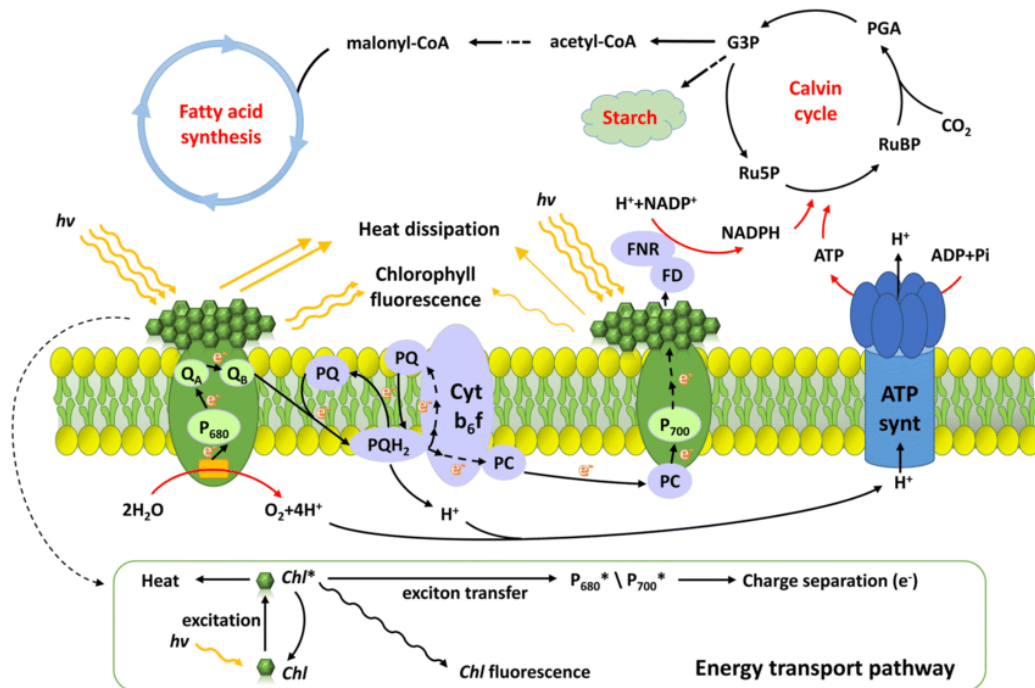


**Figure 3.** Photosynthesis mechanism scheme of its biochemical and biophysical processes (Yang et al., 2020).

The Calvin-Benson cycle is the primary pathway by which plants, algae, and cyanobacteria assimilate CO<sub>2</sub> from the atmosphere. This cycle involves a series of biochemical reactions that result in the conversion of CO<sub>2</sub> into sugars like glucose. Central to this process is the enzyme ribulose-1,5-bisphosphate carboxylase oxygenase (RuBisCO), which catalyses the carboxylation of ribulose bisphosphate to form phosphoglycerate, the first step in carbon fixation. The reduction and regeneration phases of the cycle then transform phosphoglycerate into sugars using ATP and NADPH generated during the light reactions (Ruiz-Ruiz et al., 2020b).

The global reaction is expressed as follows:



Microalgae possess a vast array of biotechnological applications due to their versatility and production of high-added value compounds. They are rich in essential nutrients such as unsaturated and omega-3 fatty acids and other compounds like vitamins, phycobiliproteins, and carotenoids, which are highly valuable for human nutrition and pharmaceutical applications (Marques et al., 2011). Microalgae are considered a promising source for biofuel production due to their high lipids accumulating properties that can later be converted into biodiesel through transesterification processes (Mutanda et al., 2020). Regarding its environmental applications, they can be used in phycoremediation to treat wastewater by removing pollutants such as phosphorus, nitrogen and heavy metals. Also, they can sequester CO<sub>2</sub> generated from anaerobic digestion systems reducing GHG emissions, or be utilized as a biological alternative to upgrade biogas into biomethane by reducing its CO<sub>2</sub> concentration (De Souza et al., 2024; Morais et al., 2020).

## 1.4. Methalgae

Co-culturing methanotrophic bacteria with microalgae (concept introduced as methalgae, van der Ha et al., 2011) presents a promising approach for converting both  $\text{CH}_4$  and  $\text{CO}_2$  into valuable biomass by coupling methane oxidation and oxygenic photosynthesis. However, there is still limited research on co-culturing methane-oxidizing bacteria and microalgae communities for the simultaneous uptake of  $\text{CH}_4$  and  $\text{CO}_2$  (Ruiz-Ruiz et al., 2020; Van Der Ha et al., 2011).

Methalgae cultures can be developed using two approaches: combining already isolated algal and methanotroph strains (bottom-up) or co-enrichment from environmental samples (top-down). The bottom-up approach allows for precise control over the initial composition of the culture by selecting strains with specific characteristics and optimizing their ratios for maximum efficiency. This method is beneficial when studying specific interactions or optimizing particular outcomes, such as  $\text{CH}_4$  consumption rates or biomass production. In contrast, top-down approaches involve growing both methanotrophs and microalgae together from the start using environmental samples. This method establishes selective pressure conditions that lead to the discovery and development of novel microbial consortia with dynamic symbiotic relationships and unique capabilities (Ruiz-Ruiz et al., 2020).

In natural systems, mixed microbial populations establish dynamic equilibria with positive, neutral, or adverse interactions, leading to robust collective properties and function distribution. By utilizing methanotrophs and microalgae in co-culture, researchers have improved nutrient recovery from wastewater, produced biomass, and explored the potential of using  $\text{CH}_4/\text{CO}_2$  mixtures as carbon sources. This synergy between both is primarily driven by the exchange of photosynthetically generated  $\text{O}_2$  from microalgae and  $\text{CO}_2$  generated during methane oxidation by methanotrophs, providing a sustainable solution to remove GHG and produce value-added compounds simultaneously (Ruiz-Ruiz et al., 2024; Roberts et al., 2020; Yun et al., 2024).

The co-culture of methanotrophs and microalgae offers several benefits, such as reducing the need for extra  $\text{O}_2$  supply and enabling the conversion of biogas into high added value products with reduced economic inputs. Oxygen produced by microalgae can be utilized by methanotrophs to convert  $\text{CH}_4$  to  $\text{CO}_2$ , creating a cycle that promotes carbon retention and  $\text{CH}_4$  conversion (Figure 4). If the mixed community also contains other non-methanotrophic bacteria, they can provide essential nutrient factors and can help alleviate toxicity from metabolic by-products, such as organic acids (Ruiz-Ruiz et al., 2020). The potential for producing bioproducts, treating wastewater, and reducing GHG emissions through the methanotroph-microalgae cooperative system has attracted significant attention, resulting in several successful studies in the last decade (Table 2).

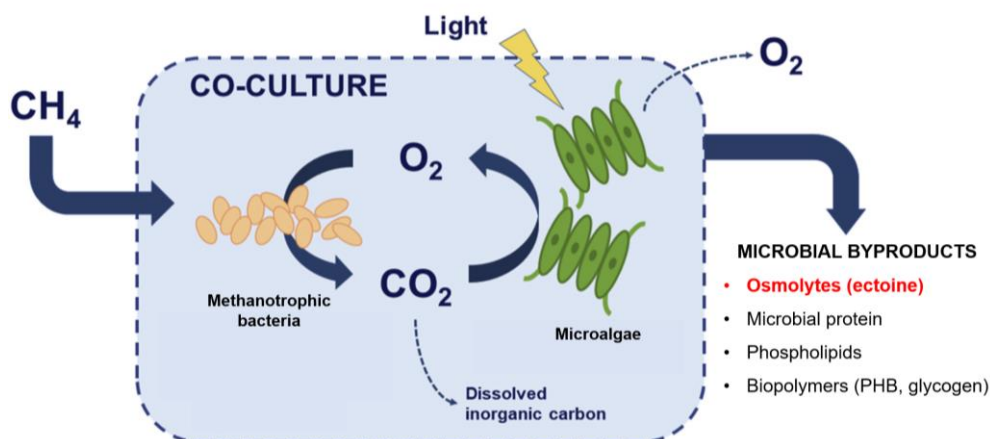


**Figure 4.** Methalgae scheme of the interaction of methanotrophs and microalgae and possible bioproducts of synthesis (adapted from Ruiz-Ruiz et al., 2020).

**Table 2.** Existing studies of the methanotroph-photoautotroph cooperative systems.

<b>Methanotrophic species</b>	<b>Photoautotrophic species</b>	<b>Cooperation mode</b>	<b>Objective</b>	<b>Result</b>	<b>Reference</b>
Methane oxidizing community	<i>Scenedesmus</i> sp.	Co-culture	Achieve sustainable CH <sub>4</sub> oxidation with no externally supplied O <sub>2</sub> . Different N sources	N source has an impact on methane oxidation	(van der Ha et al., 2011)
<i>Methylocystis parvus</i>	<i>Scenedesmus</i> sp.	Two-stage process and co-culture	Verify conversion of biogas into lipids and polyhydroxybutyrates (PHBs)	Bioproducts can be induced by N depletion. Symbiotic cooperation led to biofloc formation	(van der Ha et al., 2012)
<i>Methylomicrobium alcaliphilum</i>	<i>Synechococcus</i> sp.	Co-culture	Convert CH <sub>4</sub> and CO <sub>2</sub> into microbial protein	The co-culture technology is scalable with respect to its ability to utilize different gas streams and its biological components	(Hill et al., 2017)
<i>Methylococcus capsulatus</i>	<i>Chlorella sorokiniana</i>	Two-stage process and co-culture	Upgrade residual nutrients to single-cell protein	The protein content and amino acid profile were suitable for the substitution of conventional protein sources	(Rasouli et al., 2018)
Alkaliphilic methanotrophic consortium	<i>Scenedesmus obtusiusculus</i>	Co-culture	Greenhouse gas mitigation	Explore the effect of the initial biomass ratio and methane concentration	(Ruiz-Ruiz et al., 2020)
<i>Methylococcus capsulatus</i>	<i>Chlorella sorokiniana</i>	Co-culture	Fuels and chemical production from wastewater	The co-culture achieved 120% improvement in biomass production, 71 and 164% improvement in total nitrogen (TN) and total phosphorus (TP) removal, respectively	(Roberts et al., 2020)

<i>Methylomicrobium alcaliphilum/</i> <i>Methylococcus capsulatus</i>	<i>Synechococcus</i> sp./ <i>Chlorella sorokiniana</i>	Co-culture	Develop an experimental-computational protocol to characterize the co-culture	Obtain individual substrate consumption and product excretion rates for co-cultures	(Badr et al., 2020)
Methanotrophic consortium	Existing oxygenic photogranules	Methanotrophic granules	Aeration-free removal of dissolved methane	The syntrophy was maintained and propagated in a continuously operated reactor to remove dissolved CH <sub>4</sub>	(Safitri et al., 2021)
<i>Methylococcus/Methylosinus/Methylocystis</i>	<i>Chlorella</i> sp.	Co-culture from Waste Activated Sludge (WAS)	Effects of biogas slurry concentration, Mg <sup>2+</sup> , MOB cultivation and H <sub>2</sub> S on biogas conversion into single-cell protein (SCP)	Combined microalga and Methane oxidizing bacterial systems are less affected by higher H <sub>2</sub> S and biogas slurry	(Wang et al., 2022)
Methane oxidizing community	Photosynthetic oxygenic community	Co-culture from Waste Activated Sludge (WAS)	Iron and N source effect on growth rate, protein/lipid content and biogas conversion rate of the coculture	Higher iron availability stimulates specific growth rate, biogas conversion rate and protein/lipid content. N limitation constrains specific growth rate, and protein content without affecting lipid content	(Zhang et al., 2023)
Alkaliphilic methanotrophic consortium	<i>Scenedesmus obtusiusculus</i>	Co-culture	Biogas consumption under alkaline conditions	With pH control implementation, the co-culture exhibited a high biogas conversion with interesting biochemical composition offering potential as a microbial protein source	(Ruiz-Ruiz et al., 2024)
<i>Methylomicrobium alcaliphilum</i> 20Z	<i>Chlorella</i> sp. HS2	Co-culture	Biological methane sequestration	Explore the effect of initial methane concentration ratio and H <sub>2</sub> S concentration	(Yun et al., 2024)

Factors such as light, nutrients, temperature, pH, and mixing, play crucial roles in optimizing the cultivation conditions for these co-cultures. The pH and temperature, in particular, are critical operating parameters, due to their impact on gas dissolution and microbial metabolism (Strong et al., 2016). Community assembly associations can enhance CH<sub>4</sub>-fed bioreactors' efficiency in terms of CH<sub>4</sub> removal and bioproduct productivity. Through cooperative interactions between methanotrophs and microalgae, the production and exchange of metabolites, CO<sub>2</sub>, O<sub>2</sub> production and consumption, CH<sub>4</sub> consumption and biomass utilization can be studied and optimized for improved performance (Yun et al., 2024).

Recent research has demonstrated the potential of methanotrophs and microalgae to produce valuable intermediate bioproducts from CH<sub>4</sub> oxidation and CO<sub>2</sub> fixation. The wide range of valuable products include single-cell protein, biopolymers, like polyhydroxybutyrate (PHB), lipids, organic acids, vitamins, osmoregulators, like ectoine, and copper-binding proteins (Ruiz-Ruiz et al., 2020; Ruiz-Ruiz et al., 2024; Strong et al., 2016). One of the current main targets of research is the exploration of synergistic interactions within a microalgae-methanotroph co-culture to achieve significantly improved productivity of microbial biomass and enhanced nutrient recovery performance.

### 1.5. Ectoine

Ectoine and hydroxyectoine (Figure 5), cyclic amino acids produced intracellularly by bacteria to survive in salt-rich environments, are highly valuable products commercially produced using the halophilic Proteobacteria *Halomonas elongata* DSM 2581T. These osmoprotectant molecules play an essential role as intracellular stabilizers for nucleic acids, enzymes, and DNA-protein complexes, protecting bacteria from harsh conditions such as high temperatures, drying, freezing, and thawing, thereby resisting osmotic stress (Jawaharraj et al., 2020; Czech et al., 2018). This makes ectoine a sought-after ingredient in various industries, particularly in the cosmetic and pharmaceutical field. With a global consumption rate of around 15,000 tonnes per year and a retail value of approximately 600 to 1000 euros per kilogram (Pérez et al., 2022), depending on its purity, ectoine holds significant economic and industrial importance (Strong et al., 2016; Lim et al., 2024).

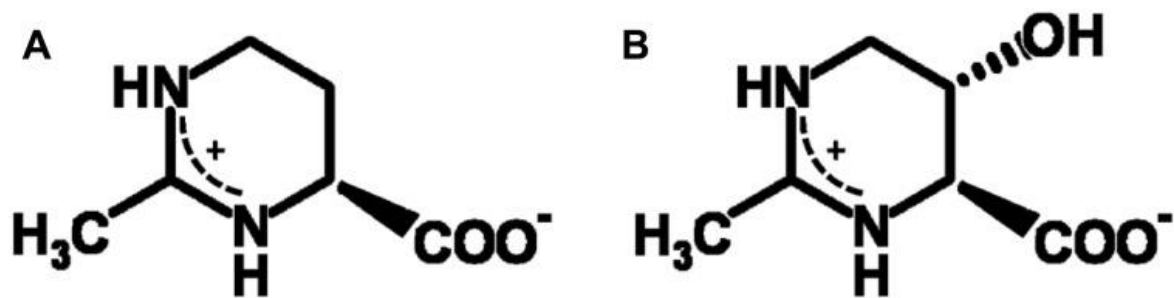


**Figure 5.** Chemical structure of ectoine (A) and hydroxyectoine (B) (Tanne et al., 2014).

From an industrial perspective, the main process currently used for ectoine production involves sugar fermentation. *Halomonas elongata*, a heterotrophic halotolerant bacterium, has been traditionally utilized commercially for ectoine production using hyperosmotic shock techniques, resulting in significant ectoine yields (Lim et al., 2024). Varying levels of ectoine production have been reported, with some strains capable of producing a benchmark of around 50-100 mg of ectoine per gram of biomass (Liu et al., 2021). This method, while effective, is costly, due to the requirement of high-quality carbon sources, such as glucose, sodium glutamate, and yeast extract.

Recent research has shown that hyperosmotic conditions enable halo-tolerant methanotrophs and methylotrophs to accumulate ectoine from diluted CH<sub>4</sub>. Currently, reported production levels using methanotrophs are usually lower than those achieved with traditional sugar-fermenting microbes. The

genetically engineered *Methylobacterium alcaliphilum* 20Z methanotroph is the highest ectoine producer among methanotrophs, with around  $1.5 \text{ g}_{\text{ectoine}} \text{ L}_{\text{culture}}^{-1}$  (Lim et al., 2024), while sugar-fermenting microbes achieve ectoine concentrations of between 10 to  $65 \text{ g}_{\text{ectoine}} \text{ L}_{\text{culture}}^{-1}$  from glucose (Cho et al., 2022).

In nature, several methanotrophs, including *Methylobacterium alcaliphilum*, *Methylobacter marinus*, *Methylobacterium kenyens*, *Methylophaga thalassica*, *Methylophaga alcalica*, and *Methylarcula marina*, have been identified as ectoine producers. These organisms contain key ectoine biosynthetic genes, including diaminobutyric acid (DABA) acetyltransferase, DABA aminotransferase, and ectoine synthase. Moderately halotolerant methanotrophs are capable of accumulating up to 12-20% of their dry mass as ectoine, making them valuable candidates for ectoine production (Jawaharraj et al., 2020; Strong et al., 2016). While methanotroph-based ectoine production currently lags behind traditional sugar-based fermentation processes, the combined process of ectoine production and the treatment of atmospheric  $\text{CH}_4$  emissions can reduce costs associated with ectoine production and contribute to climate change mitigation through active  $\text{CH}_4$  reduction. This approach aims to bridge the gap between the two methods (Lim et al., 2024; Strong et al., 2016).

The utilization of methanotrophs for ectoine production offers a sustainable and environmentally friendly approach to meet the growing demand for this valuable compound. By leveraging the unique capabilities of methanotrophs to convert  $\text{CH}_4$  into ectoine, we can not only reduce the costs associated with traditional ectoine production, but also contribute to climate change mitigation efforts. As research in this field continues to evolve, methanotroph-based ectoine production holds immense potential for revolutionizing the cosmetics and biotechnology industries while driving sustainable practices in microbial production processes (Lim et al., 2024). By coupling these microorganisms with microalgae in syntrophic systems, the overall  $\text{CH}_4$  and  $\text{CO}_2$  abatement, while producing valuable metabolites such as ectoine, can be achieved (Ruiz-Ruiz et al., 2020).

Currently, there is no existing information supporting the production of ectoine from microalgae (Table 3). As far as the author knows, there are no ongoing studies investigating the levels of ectoine in mixed cultures of microalgae and methanotrophs using biogas as carbon/energy source. Hence, this master's thesis represents a pioneering attempt in this field.

**Table 3.** Previous studies on ectoine production from biogas by methanotrophic or microalgae systems.

<b>Methanotrophic species</b>	<b>Photoautotrophic species</b>	<b>Type of culture</b>	<b>Objective</b>	<b>Results</b>	<b>Reference</b>
Consortium from salt lagoon	-	Mixed	Optimize operational conditions for ectoine production in a pilot-scale bubble reactor and subsequent extraction through bio-milking process.	Higher N and CH <sub>4</sub> loading rates increased CH <sub>4</sub> degradation but did not result in higher ectoine concentrations. Osmotic shocks allowed a quick (<5 min) release of ectoine into the medium under lower salinity conditions.	(Rodero et al. 2023)
Consortium from salt lagoon	-	Mixed	Assess the influence of biomass concentration, Cu <sup>2+</sup> , Mg <sup>2+</sup> , N source (ammonium and nitrate), CH <sub>4</sub> content in biogas and NaCl concentration in a pilot-scale bubble column bioreactor to optimize these conditions.	<ul style="list-style-type: none"><li>- Lower biomass concentrations resulted in higher specific ectoine yields (42 mg<sub>ectoine</sub> g<sub>TSS</sub><sup>-1</sup>).</li><li>- Nitrate was a more effective N source than ammonium.</li><li>- Cu<sup>2+</sup> and Mg<sup>2+</sup> variations did not have a significant impact on ectoine production or process performance.</li><li>- Increase in CH<sub>4</sub> content enhanced methane removal but does not improve ectoine yields.</li><li>- Lower NaCl concentrations enhanced methane biodegradation but decreased ectoine yield.</li></ul>	(Rodero et al. 2022)
<i>Methylophilum</i> <i>alcaliphilum</i>	-	Mixed	Evaluate the potential of biogas as a raw material for ectoine production and its accumulation efficiency.	Biogas usage resulted in a 3 to 6-fold decrease in production costs compared to traditional industrial processes. This culture produced up to 109 mg <sub>ectoine</sub> g <sub>TSS</sub> <sup>-1</sup>	(Cantera et al., 2020)
Mixed haloalkaliphilic consortium	-				



-	<i>Thalassiosira weissflogii</i> <i>Phaeodactylum tricorutum</i>	Axenic (Bottom-up approach)	Identify ectoine in microalgae species and determine if its origin is microalgal or from its associated bacteria.	Ectoine is a relevant osmoadaptive metabolite in phytoplankton produced by its associated bacteria.	(Fenizia et al., 2020)
<i>Methylomicrobium alcaliphilum</i> 20Z and mixed haloalkaliphilic consortium	-	Mixed	Demonstrate the feasibility of CH <sub>4</sub> biorefinery concept for simultaneously producing multiple high-value metabolites (ectoine, hydroxyectoine, PHAs and EPS) using methane as sole carbon and energy source.	High Mg <sup>2+</sup> promoted ectoine accumulation (79.7-94.2 mg <sub>ectoine</sub> g <sub>TSS</sub> <sup>-1</sup> ), hydroxyectoine (13 mg g <sub>TSS</sub> <sup>-1</sup> ) and EPS (2.6 g L <sup>-1</sup> ). PHA synthesis was almost negligible	(Cantera et al. 2018)
<i>Methylomicrobium alcaliphilum</i> 20Z	-	Axenic	Demonstrate that the strain 20Z can efficiently synthesize and excrete ectoine using methane as sole carbon and energy source through a bio-milking process.	20Z had a rapid response to osmotic shocks by releasing accumulated ectoine under low salinity and retaking it during high salinity osmotic shocks. Lower intracellular ectoine concentration (70.4 ± 14.3 mg <sub>ectoine</sub> g <sub>TSS</sub> <sup>-1</sup> ) than other bacterial species but with higher environmental performance.	(Cantera et al. 2017)
<i>Methylomicrobium alcaliphilum</i> 20Z	-	Axenic	Couple ectoine production with CH <sub>4</sub> abatement. Assess the effect of Cu <sup>2+</sup> , temperature, NaCl and CH <sub>4</sub> concentration in the production of ectoine and CH <sub>4</sub> abatement.	The highest intracellular ectoine production yields were recorded at elevated CH <sub>4</sub> concentrations with low NaCl levels (31.0 ± 1.7 mg <sub>ectoine</sub> g <sub>biomass</sub> <sup>-1</sup> ), or at low CH <sub>4</sub> concentrations combined with high NaCl levels (66.9 ± 4.2 mg <sub>ectoine</sub> g <sub>biomass</sub> <sup>-1</sup> ). Additionally, extracellular ectoine was detected at high Cu <sup>2+</sup> concentrations, indicating that the methanotroph had the ability to excrete it.	(Cantera et al. 2016)

## 2. OBJECTIVES

The EctoMet FWO funded project, a collaboration between UGent, KU Leuven and VITO, aims to establish a novel, sustainable methalgae platform for the production of high-value chemicals, more specifically ectoine, through the complete valorisation of biogas (both CO<sub>2</sub> and CH<sub>4</sub>). The project is divided into four Work Packages (WP) to work towards this objective (Figure 6). This master thesis is framed into WP1: the establishment of a co-enrichment from natural environments, following a top-down approach, to maximize the potential of finding a suitable methalgae consortium as a reliable ectoine producer for its subsequent scaling up.

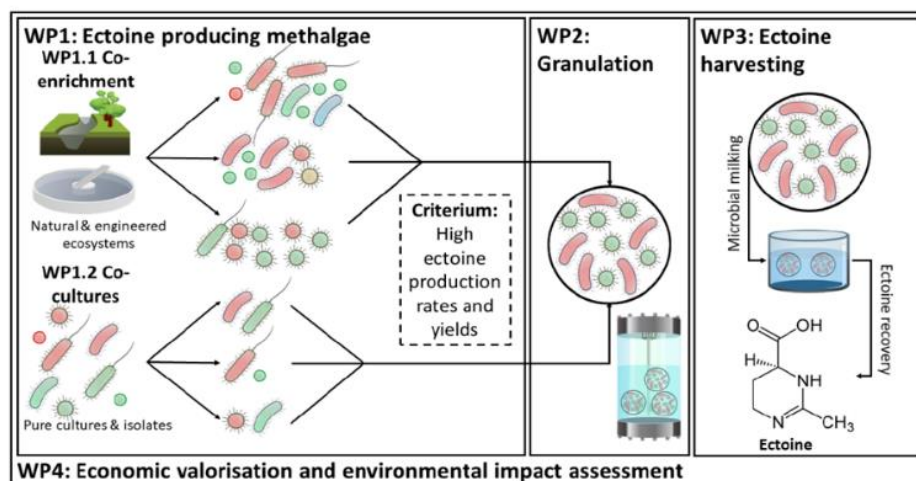


**Figure 6.** Schematic overview of the EctoMet project and its Work Packages (WP). Green microorganisms depict microalgae, red methanotrophs, blue and yellow satellite species.

The aim of this master thesis is to achieve a sustainable and carbon neutral methane oxidation process from biogas with reduced need for externally supplied O<sub>2</sub> for the production of ectoine via a top-down approach. This novel strategy starts with the enrichment of microbial communities from natural environments to identify key species involved in this process followed by enhancing salinity parameters to increase ectoine production. In this study, the adaptability of the cultivated communities and their ectoine yield when exposed to intermittent osmotic stress, with the intention of further increasing its ectoine content, will be evaluated. The outcomes of this study will provide a first attempt towards the development of a production system for ectoine synthesis from natural enrichments from the North Sea samples with synthetic biogas streams. To fulfil this, the following subobjectives were defined:

- Enrichment of methanotroph-microalgae consortia from natural environments;
- Selection of optimal salinity concentrations to maximize biomass growth and ectoine production;
- Evaluation of culture resilience and ectoine synthesis under periodic osmotic shocks.

### 3. MATERIALS AND METHODS

#### 3.1. Experimental outline

Figure 7 provides an overview of all the experimental work conducted throughout this master's thesis to present a comprehensive view of the entire process. Four samples from the North Sea were sourced and enriched in serum bottles for 10 weeks under selective conditions to promote a mixed culture containing methanotrophic bacteria and microalgae. The enrichment with the highest CH<sub>4</sub> removal efficiency (RE) was selected as inoculum for further experiments. These experiments aimed to determine the most suitable NaCl concentration for methalgae culture growth and ectoine production, as well as to depict its behaviour under various osmotic shock stresses (Figure 7).

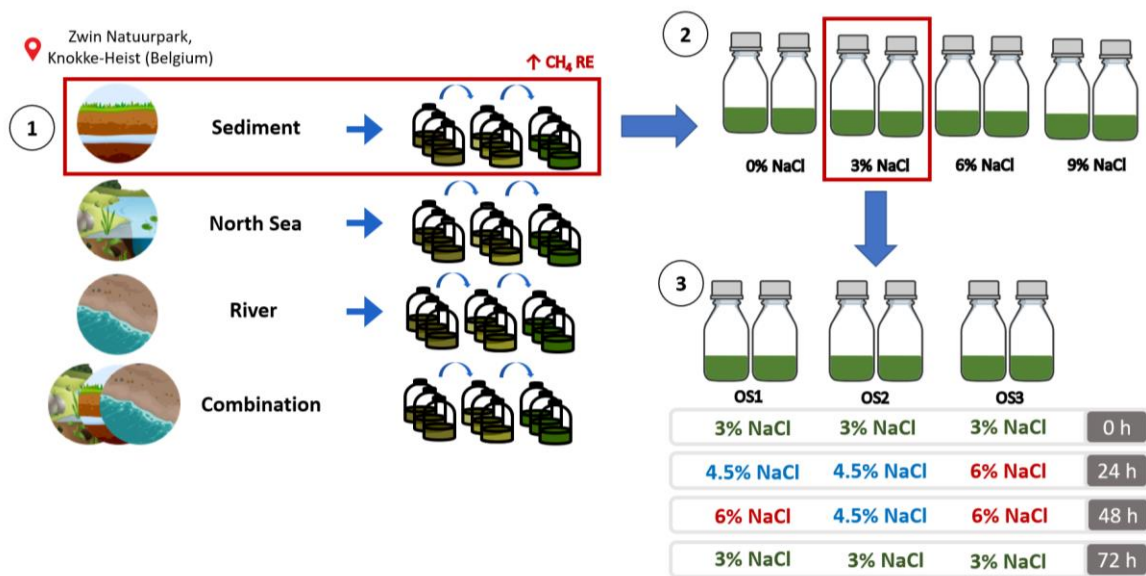


**Figure 7.** Overview of the experimental work performed during this master thesis. 1) Selection of the methalgae enrichment that presented the highest CH<sub>4</sub> removal efficiencies, 2) determination of most suitable NaCl concentration for the methalgae growth and 3) evaluation of the culture performance under different osmotic shock stress conditions.

#### 3.2. Enrichments from a saline environment

##### 3.2.1. Sampling site description

For the methanotrophic bacteria and microalgae enrichments, three sampling points from the Zwin Natuur Park, a nature reserve on the North Sea coast on the Belgian-Dutch border, were sourced on the 22<sup>nd</sup> November of 2023 (Figure 8, Table 4). Sampling point's main characteristics are described in Table 4.

Zwin Natuurpark  
Knokke-Heist

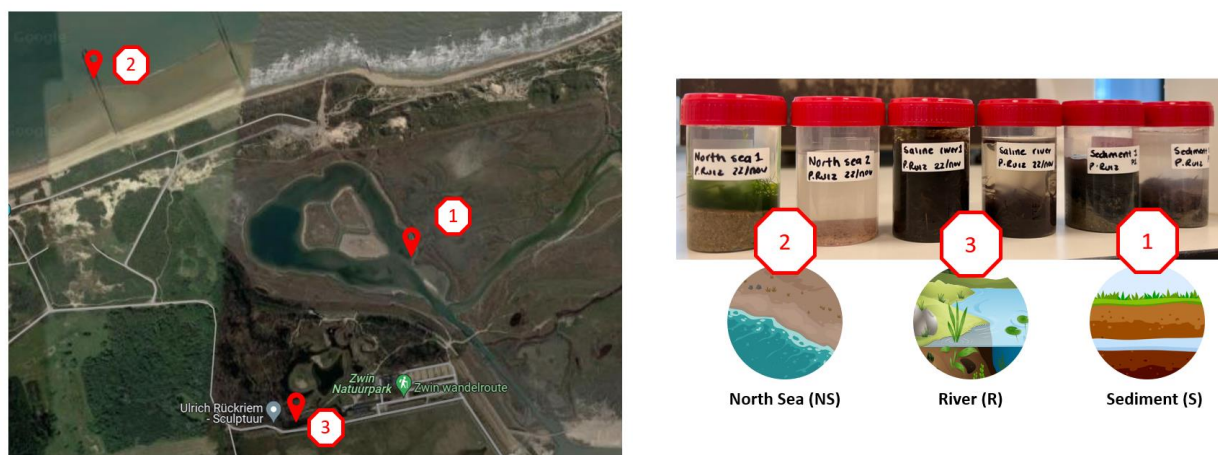


**Figure 8.** Site, sampling points and samples.

**Table 4.** Site characteristics and sample initial characterization.

Sample name	Place of sampling	Coordinates	Water temperature	Water pH	Water salinity	Initial optical microscope observations
Sediment	North Sea swamp coast sediment (1)	5 1°21'38.0"N 3°21'09.8"E		7.43	3%	Presence of few diatoms and cyanobacteria
River	River sediment (3)	5 1°21'28.9"N 3°20'45.9"E	15.3°C	7.7	0.2-2%	Great diversity of filamentous cyanobacteria, green microalgae and a few diatoms
North Sea	Salty water of the North Sea (2)	51°21'56.6"N 3°20'21.9"E		7.86	3%	Great diversity of diatoms, green microalgae and cyanobacteria

### 3.2.2. Culture conditions

The samples, designated Sediment (S), North Sea (NS), River (R), and a Combination of these three (C), were enriched in 120 mL transparent serological bottles with butyl septa and aluminium caps. Initially, 2 grams of combined soil and water from the sampling points were added to 20 mL of sterile mineral salt medium (MSM) (Table 5) with nitrate (NO<sub>3</sub><sup>-</sup>) as main N source. A concentration of 3% NaCl was used for all the methalgae enrichments. Pure CH<sub>4</sub> was injected into the headspace using a 60 mL syringe (with <10% CH<sub>4</sub> in air to avoid explosive atmosphere), as the only carbon source, immediately after removing an equivalent volume of air to prevent overpressure in the glass bottles and always ensuring a 1:1.5 CH<sub>4</sub>:O<sub>2</sub> volume ratio.

The headspace gas composition was renewed every 2 days, with initial and final CH<sub>4</sub>, O<sub>2</sub>, and CO<sub>2</sub> concentrations monitored by GC-TCD (as described in section 3.5.1.). Every two weeks, 2 mL aliquots from the previous enrichment were sequentially transferred to new sterile serological bottles, containing

18 mL of fresh MSM with 3% NaCl, over a total period of 10 weeks. The bottles were incubated in an orbital shaker at 125 rpm in a controlled temperature room ( $28 \pm 2$  °C). Full-spectrum LED lights were placed above the orbital shaker to provide an average irradiance of  $120 \mu\text{mol m}^{-2} \text{s}^{-1}$ . Enrichments were performed in duplicates. The enrichments that showed minimal or no  $\text{CH}_4$  removal capacity were discontinued before the 10 weeks to prevent wasting resources. The methalgae enrichment that presented the highest  $\text{CH}_4$  removal efficiencies was selected for the next experiments.

**Table 5.** Mineral salts medium composition without additional NaCl.

<b>Nutrient</b>	<b>Concentration (g L<sup>-1</sup>)</b>
Magnesium sulphate heptahydrate ( $\text{MgSO}_4 \cdot 7\text{H}_2\text{O}$ )	1
Potassium nitrate ( $\text{KNO}_3$ )	1
Calcium chloride dihydrate ( $\text{CaCl}_2 \cdot 2\text{H}_2\text{O}$ )	0.15
FeNaEDTA	0.0005
Sodium phosphate dibasic dodecahydrate ( $\text{Na}_2\text{HPO}_4 \cdot 12\text{H}_2\text{O}$ )	0.717
Potassium dihydrogen phosphate ( $\text{KH}_2\text{PO}_4$ )	0.272
<b>Trace elements</b>	<b>Concentration (mg L<sup>-1</sup>)</b>
$\text{Na}_2\text{EDTA} \cdot 2\text{H}_2\text{O}$	0.5
Ferrous sulphate heptahydrate ( $\text{FeSO}_4 \cdot 7\text{H}_2\text{O}$ )	0.2
Boric acid ( $\text{H}_3\text{BO}_3$ )	0.03
Cobalt(II) chloride ( $\text{CoCl}_2 \cdot 6\text{H}_2\text{O}$ )	0.02
Zinc sulphate ( $\text{ZnSO}_4 \cdot 7\text{H}_2\text{O}$ )	0.01
Manganese(II) chloride tetrahydrate ( $\text{MnCl}_2 \cdot 4\text{H}_2\text{O}$ )	0.003
Sodium molybdate dihydrate ( $\text{NaMoO}_4 \cdot 2\text{H}_2\text{O}$ )	0.003
Nickel(II) chloride hexahydrate ( $\text{NiCl}_2 \cdot 6\text{H}_2\text{O}$ )	0.002
Copper(II) sulphate pentahydrate ( $\text{CuSO}_4 \cdot 5\text{H}_2\text{O}$ )	2

pH = 6.8

### 3.3. Salinity test: Influence of NaCl concentration on growth, ectoine production and gas consumption

The selected enriched methalgae, based on the highest  $\text{CH}_4$  removal efficiency, was pre-grown in a 1 L gas-tight reactor for 7 days to produce enough inoculum for this experiment, following the same culture conditions as described in section 3.2.2. To study the influence of different NaCl concentrations, 20 mL of the enriched methalgae inoculum and 180 mL of MSM with NaCl concentrations of 0%, 3%, 6%, and 9% were carried out in 0.6 L gas-tight reactors in biological duplicates on the growth performance of co-cultures,  $\text{CH}_4$  removal efficiency and methanotroph-microalgae ratios. The headspace gas composition, ensuring a 1:1.5  $\text{CH}_4$ : $\text{O}_2$  volume ratio, was renewed every 2 days, with initial and final  $\text{CH}_4$ ,  $\text{O}_2$ , and  $\text{CO}_2$  concentrations monitored by GC-TCD (as described in section 3.5.1).

The gas tight reactors were incubated in an orbital shaker at 125 rpm in a controlled temperature room ( $28 \pm 2$  °C). Full-spectrum LED lights were placed above the orbital shaker to provide an average constant irradiance of  $120 \mu\text{mol m}^{-2} \text{s}^{-1}$ . The reactors were randomly distributed in the shaker after every replenishment to reduce the impact of light incidence and gas-liquid mass transfer variabilities in the experiment. Liquid samples were drawn at the beginning and end of the experiment to measure ectoine, TSS (Total Suspended Solids), VSS (Volatile Suspended Solids), and cell density and size characteristics through flow cytometry (FCM). Experiment duration was 14 days.

### 3.4. Osmotic shock tests

The selected enriched methalgae was pre-grown in a 1 L gas-tight reactor for 7 days to produce enough inoculum for this experiment, following the same culture conditions as described in section 3.2.2. To study the osmotic shock that different concentrations of NaCl induces in ectoine accumulation, experiments were carried out in 0.6 L reactors in biological duplicates using 20 mL of methalgae

inoculum and 120 mL of MSM. The osmotic shock experiment lasted for a total of 5 days, consisting of 2 days for acclimating the cultures to 3% NaCl in the bioreactors, followed by 2 days of osmotic testing, and concluding with 1 day of returning the culture to 3% NaCl conditions. The experimental conditions and duration are presented in Table 6.

**Table 6.** Percentage of NaCl over the experimental time in the three osmotic shock tests conducted: OS1, OS2 and OS3.

Treatment	Time (h)			
	0	24	48	72
OS1	3%	4.5%	6%	3%
OS2	3%	4.5%	4.5%	3%
OS3	3%	6%	6%	3%

The bottles were incubated in an orbital shaker at 125 rpm in a controlled temperature room ( $28 \pm 2$  °C). Full-spectrum LED lights were placed above the orbital shaker to provide an average irradiance of  $120 \mu\text{mol m}^{-2} \text{s}^{-1}$ . The headspace gas composition (synthetic biogas), ensuring a 1:1.5:0.6 CH<sub>4</sub>:O<sub>2</sub>:CO<sub>2</sub> volume ratio, was renewed every 2 days, with initial and final CH<sub>4</sub>, O<sub>2</sub>, and CO<sub>2</sub> concentrations monitored by GC-TCD (as described in section 3.5.1). By formulating a synthetic biogas mixture, instead of utilizing biogas from an anaerobic digester, it allowed to avoid impurities like H<sub>2</sub>S, which can have an adverse effect on biomass production and removal efficiencies, and also to provide better control over the biogas composition. The reactors were randomly distributed in the shaker after every replenishment to reduce the impact of light incidence and gas-liquid mass transfer variabilities in the experiment. Before every osmotic shock, the biomass was sedimented by centrifugation in 50 mL tubes for 10 min at maximum speed (7830 rpm), discarding the supernatant and resuspending the pellet with 140 mL of fresh MSM to ensure that there were no nutrient limitations affecting the cultures. The entire medium replacement process took approximately 3 hours to complete before the cultures were fully restored. Initial and final gas samples were taken to measure CH<sub>4</sub>, O<sub>2</sub>, and CO<sub>2</sub> concentrations by GC-TCD. Initial and final liquid samples were also drawn every day to measure TSS/VSS, ectoine concentration and cell density through FCM.

### 3.5. Analytical techniques

#### 3.5.1. Gas chromatography (GC)

The gas phase composition was analysed with a Compact GC4.0 (Global Analyser Solutions, Breda, The Netherlands), equipped with a Molsieve 5A pre-column and Porabond Q column (CH<sub>4</sub>, O<sub>2</sub>, H<sub>2</sub> and N<sub>2</sub>) and a Rt-Q-bond pre-column and column (CO<sub>2</sub>, N<sub>2</sub>O and H<sub>2</sub>S). Concentrations of gases were determined by means of a thermal conductivity detector (TCD) with a minimum detection limit of 100 ppmv for each gas.

#### 3.5.2. Microbial growth

Total suspended solids (TSS) and volatile suspended solids (VSS) concentrations were measured according to standard methods 2540 D and 2540 E (American Public Health Association, 1998) using glass fibre membrane filters, with a 0.3  $\mu\text{m}$  pore size. To calculate TSS and VSS, the mass (in g) and volume of sample (mL) are converted to  $\text{g L}^{-1}$  by using equations (3) and (4), respectively.

$$TSS (\text{g/L}) = \frac{\text{mass}_{\text{filter after } 105^{\circ}\text{C (sample)}} (\text{g}) - \text{mass}_{\text{initial filter (no sample after } 550^{\circ}\text{C)}} (\text{g})}{\text{volume of sample (L)}} \quad (3)$$

$$VSS (\text{g/L}) = \frac{\text{mass}_{\text{filter after } 550^{\circ}\text{C (sample)}} (\text{g}) - \text{mass}_{\text{filter after } 105^{\circ}\text{C (sample)}} (\text{g})}{\text{volume of sample (L)}} \quad (4)$$

### 3.5.3. pH

All liquid samples pH measurements were carried out manually with a micro pH electrode (Consort C3210 Multi-parameter analyser, Belgium) to monitor the process and considering it for gas concentration calculations. The pH metre was calibrated with pH 4, pH 7 and pH 10 solutions before each use.

### 3.5.4. Ectoine

As depicted in figure 9, biomass samples were concentrated 3-fold by centrifugation of 2 mL of the culture broth at 13,000 g for 5 min in a cryotube, and pellets were stored at -20 °C until further intracellular ectoine extraction. An aliquot of 1.5 mL of a solution of 80% ethanol and 20 ± 5 mg of 0.1 mm diameter zirconia/glass beads (Biospec Products, Belgium) was added to the tube followed by cell disruption in a PowerLyzer (Mo Bio Laboratory Inc., USA) at 2000 rpm for 10 min. The supernatant was kept at 4 °C overnight, and the suspension was centrifuged at 13,000 g for 5 min and filtered through 0.22 µm filters prior to analysis by HPLC-UV. Commercial ectoine (≥95.0%, Sigma Aldrich) was used as for calibration curve preparation and as a standard during sample analysis. Ectoine was analysed by HPLC-UV using an Aminex HPX-87C column (Bio-Rad Laboratories, USA), with CaCl<sub>2</sub> (5 mM) as the eluent and detection at 210 nm (Onraedt et al., 2004). The flow was 0.5 mL min<sup>-1</sup> with a UV detection point at 210 nm; the column temperature was 85 °C and the runtime 52 min per sample, with a detection point for ectoine in minute 47. For extracellular ectoine content determination, the supernatant of the culture after the initial sample centrifugation was stored without requiring additional extraction steps. It was only necessary to filter it through a 0.22 µm filter before conducting HPLC-UV analysis to maintain the column's integrity.

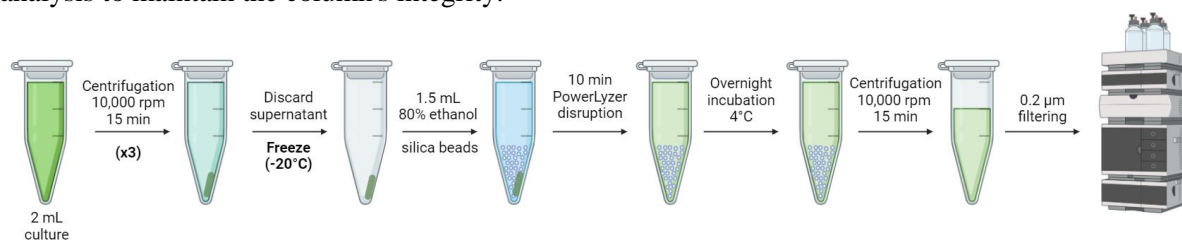


**Figure 9.** Intracellular ectoine extraction and measurement protocol.

### 3.5.5. Flow cytometry

To measure the total number of cells, a flow cytometer (Attune NxT, FCM) was used. A sample of 180 µL, previously sonicated for 3 min to disaggregate culture granules, was placed in 96 well-plates in triplicates. Samples for flow cytometry measurement were prefiltered with 20 µm pore size filters to avoid clogging the cytometer and diluted in series (10x, 100x, and 1000x) to ensure the samples contained no more than 10<sup>6</sup> cells mL<sup>-1</sup>. This ensured that particles could pass by the laser and detectors one by one providing an accurate cell count. Then, 1% volume of SYBR Green stain was added to the sample and incubated at 37 °C for 20 min to stabilize. The staining characteristics and procedure were established considering that samples came from mixed cultures of methanotrophs, heterotrophic bacteria and microalgae, where SYBR Green staining during a longer incubation period than usual for isolated strains would effectively stain their nucleic acids. The samples were analysed using the Blue laser, first detector (BL1), and Forward Scatter (FSC) channels, ensuring the measurements ranged from 200 to 2000 events per second to avoid background noise interference when analysing the data. The use of BL1 and FSC channels help in distinguishing and characterizing microalgae and methanotroph cultures cells based on their size, complexity, and fluorescence properties. BL1 is particularly useful for detecting chlorophyll and other pigments in microalgae while FSC helps to differentiate between different types of microorganisms based on their size.

After the samples were analysed, control samples of the medium without any biomass (filtered with a 0.22 µm filter) were used to identify the background noise and gate it to distinguish it from the methanotroph (bacteria)-microalgae cells. The cell counting and differentiation were performed by first removing the background and then gating.

Flow cytometry was chosen over Neubauer counting chamber due to the more effectively differentiation between small cells in the mixed culture, as both microalgae and methanotrophs size ranges between 0.7 to 2 µm. Additionally, it provides more accurate results in comparison to manual counting.

### 3.6. Molecular characterization

The DNA extraction from the enriched culture was carried out using the PowerSoil DNA Isolation Kit<sup>TM</sup>, according to the manufacturer's instructions, followed by a DNA amplification through PCR using Phusion Plus Green PCR Master Mix<sup>TM</sup> for eukaryotic and prokaryotic organisms.

The genomic DNA extract was sent out to LGC genomics GmbH (Berlin, Germany) for library preparation and sequencing. Sequencing was performed via Illumina Miseq platform with V3 chemistry. Primers 341F (5'-CCTACGGGNGGCWGCAG -3') and 785Rmod (5'-GACTACHVGGGTATCTAA KCC-3') (Klindworth et al., 2013) targeting the V4 region of the 16S rRNA gene were used for the bacteria domain and primers TAREuk454FWD1 (5'-CCAGCA(G/C)C(C/T)GCGGTAA TTCC-3') and TAREukREV3 (5'-ACTTTCGTTCTTGAT(C/T)(A/G)A-3') targeting the V4 region of the 18S rRNA gene (Stoeck et al. 2010) were selected for targeting the eukaryotic microalgae.

Illumina amplicon sequence data results were processed with DADA2 R package. Primer sequences were removed, and reads were truncated at a quality score cut-off (truncQ=2). Besides trimming, additional filtering was performed to eliminate reads containing any ambiguous base calls or reads with high expected errors (maxEE=2,2). After dereplication, unique reads were further denoised using the Divisive Amplicon Denoising Algorithm (DADA) error estimation algorithm and the selfConsist sample inference algorithm (with the option pooling =TRUE). The obtained error rates were inspected and after approval, the denoised reads were merged. An additional clean-up step was implemented, when the total amount of target over all samples was lower or equal to 1, the amplicon sequence variant (ASV) was removed. Finally, the ASV table obtained after chimera removal was used for taxonomy assignment using the Naive Bayesian Classifier and the DADA2 formatted Silva v138.1 (Quast et al 2013).

### 3.7. Calculations and statistical analysis

To quantify the amount of CH<sub>4</sub>, O<sub>2</sub> or CO<sub>2</sub> consumed or produced, the removal efficiency percentage (RE) was calculated by subtracting the initial replenishment gas concentration from the final exhaust gas concentration and dividing it by the initial replenishment gas concentration as follows:

$$RE (\%) = \frac{[gas]_{initial} (\%) - [gas]_{final} (\%)}{[gas]_{initial} (\%)} \cdot 100 \quad (5)$$

A statistical analysis was conducted to evaluate the effect of varying salinities on CH<sub>4</sub> removal efficiency and ectoine production. For each experiment, average values were calculated from biological duplicates of each experimental condition, along with their standard deviations, to provide a clear and concise data summary. A Pearson test was used to assess whether the dataset followed a normal



distribution, resulting in a p-value greater than 0.05. If the data exhibited normal distribution and homoscedasticity, t-tests or ANOVA were used to compare the impact of different variables on the experimental groups. Otherwise, the Mann-Whitney U test was applied to compare non-parametric data between two samples and Kruskal-Wallis test to compare more than two independent samples, as they do not assume normality and can accommodate unequal sample sizes. All statistical analyses were performed using the IBM SPSS Statistics (Version 25) software.

## 4. RESULTS

### 4.1. Enrichments from saline environments

#### 4.1.1. Gas evolution in the enrichments

Figure 10 illustrates that the Sediment enrichment exhibited higher and more consistent  $\text{CH}_4$  oxidation and  $\text{CO}_2$  production compared to the other three samples. This enrichment maintained a more dynamic equilibrium as all the  $\text{CH}_4$  in the headspace was rapidly consumed and oxidized into  $\text{CO}_2$  by the methanotrophs, while a portion of this  $\text{CO}_2$  was subsequently fixed by the microalgae. This fixation through photosynthesis produced  $\text{O}_2$ , ensuring that the reactor never became completely anoxic, as clearly shown in graph A of Figure 10. In contrast, the River and North Sea enrichments barely showed  $\text{CH}_4$  oxidation, resulting in no  $\text{O}_2$  consumption or  $\text{CO}_2$  production. Moreover, microalgal activity was not apparent in these two enrichments, as indicated by the absence of  $\text{O}_2$  production and  $\text{CO}_2$  fixation. The Combination enrichment exhibited fluctuating gas production and consumption rates throughout the experiment, with  $\text{CH}_4$  removal efficiencies below 20% between days 15 and 31. Due to this poor oxidation, any  $\text{CO}_2$  produced was quickly fixed by microalgae, leading to consistently zero  $\text{CO}_2$  levels in the headspace during each sampling. Enrichments that did not demonstrate clear  $\text{CH}_4$  removal were discontinued earlier to avoid wasting of resources, starting with the North Sea enrichment after 4 weeks, the River enrichment after 6 weeks, and the Combination enrichment after 8 weeks.

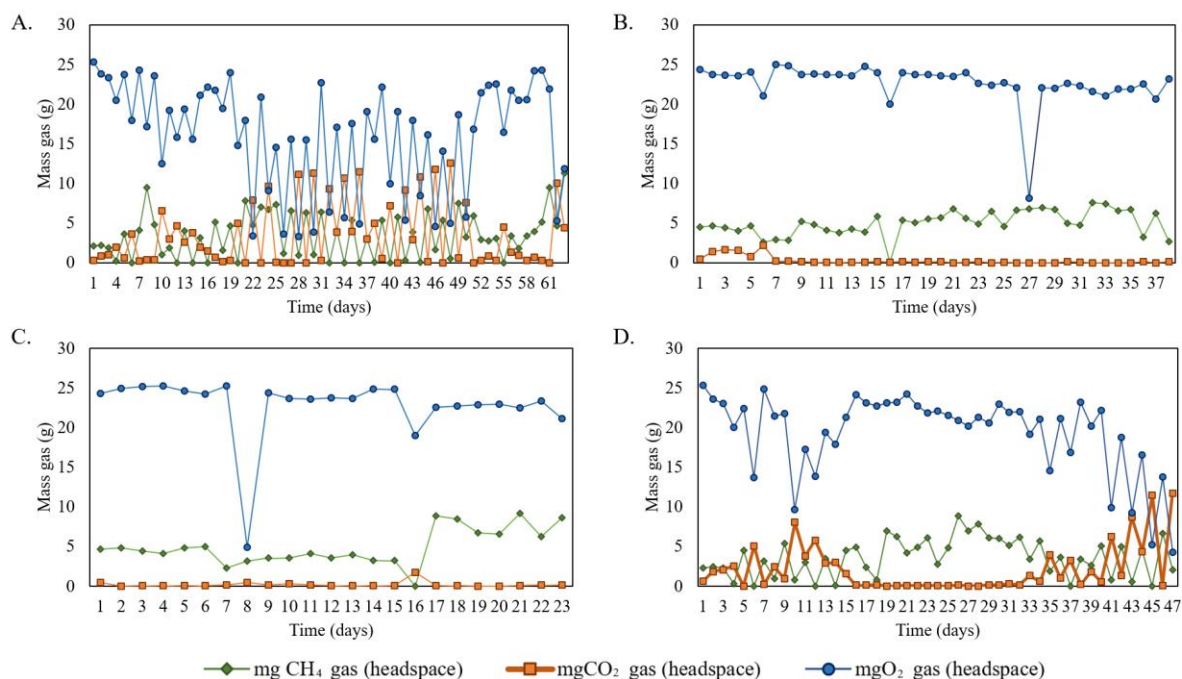


**Figure 10.** Amount of methane ( $\text{CH}_4$ ), oxygen ( $\text{O}_2$ ) and carbon dioxide ( $\text{CO}_2$ ) in milligrams (mg) in the headspace of the serum bottles during the enrichment period for the four different North Sea samples shown as: A) Sediment (10 weeks incubation). B) River (6 weeks incubation). C) North Sea (4 weeks incubation). D) Combination (8 weeks incubation).

### 4.1.2. Methane removal efficiencies

Figure 11 reveals a distinct difference in CH<sub>4</sub> removal efficiencies between the Sediment and Combination enrichments compared to the North Sea and River enrichments, with the latter showing significantly lower CH<sub>4</sub> removal efficiencies (Kruskal-Wallis test,  $p < 0.001$ ). Of the two most efficient enrichments, Sediment demonstrated a higher and more consistent average CH<sub>4</sub> removal efficiency of  $87.7 \pm 16.5\%$  compared to the River, North Sea, and Combination samples (Figure 11). Although the overall CH<sub>4</sub> removal efficiencies of the Sediment and Combination enrichments are similar, statistical analysis indicates a significant difference in their performance (Mann-Whitney U test,  $p = 0.033$ ). Consequently, Sediment was selected as the most optimal enrichment for further experiments focused on biomass growth and ectoine production.

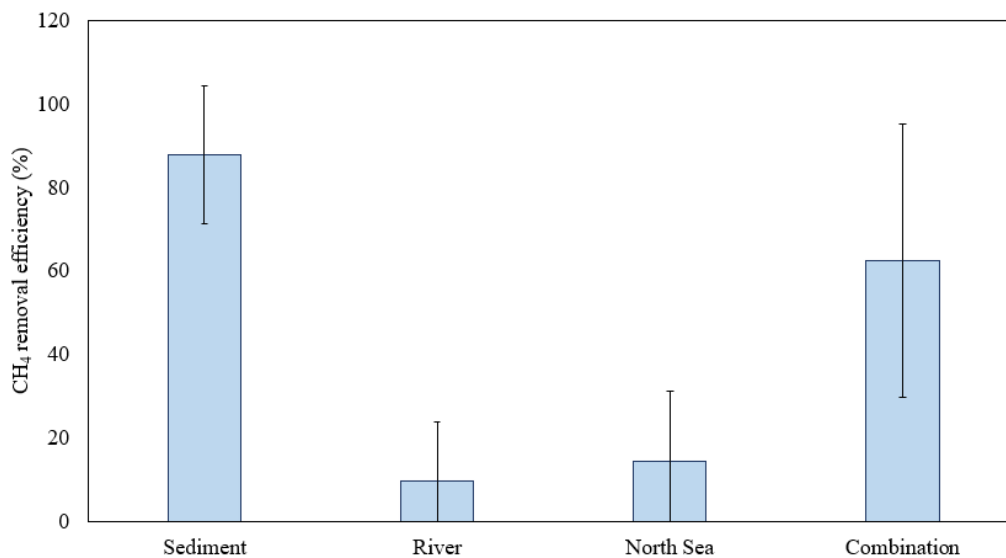


**Figure 11.** Average CH<sub>4</sub> removal efficiency per 2-day replenishment for each enrichment during the entire incubation period. The error bars indicate the standard deviation of each value.

### 4.1.3. Microbial composition

The 16S and 18S rRNA gene Illumina amplicon sequence revealed the microbial composition and relative abundance (Figure 12) of the Sediment enrichment. *Picochlorum oklahomense* was the predominant photosynthetic eukaryotic microorganism with a 97% relative abundance, followed by *Nannochloris* sp. with less than 1% relative abundance. The prokaryotic composition was more diverse, including halophilic methylotrophic and heterotrophic microorganisms. The methanotroph *Methylobacter marinus/whittenburyi* and the methylotroph *Methylophaga marina* comprised 10% and 5% of the culture, respectively, followed by halophilic heterotrophic bacteria such as *Labrenzia* sp., *Labrenzia aggregate* and *Hyphomonas adhaerens*. The characteristics of the main species are enlisted in Table 7.

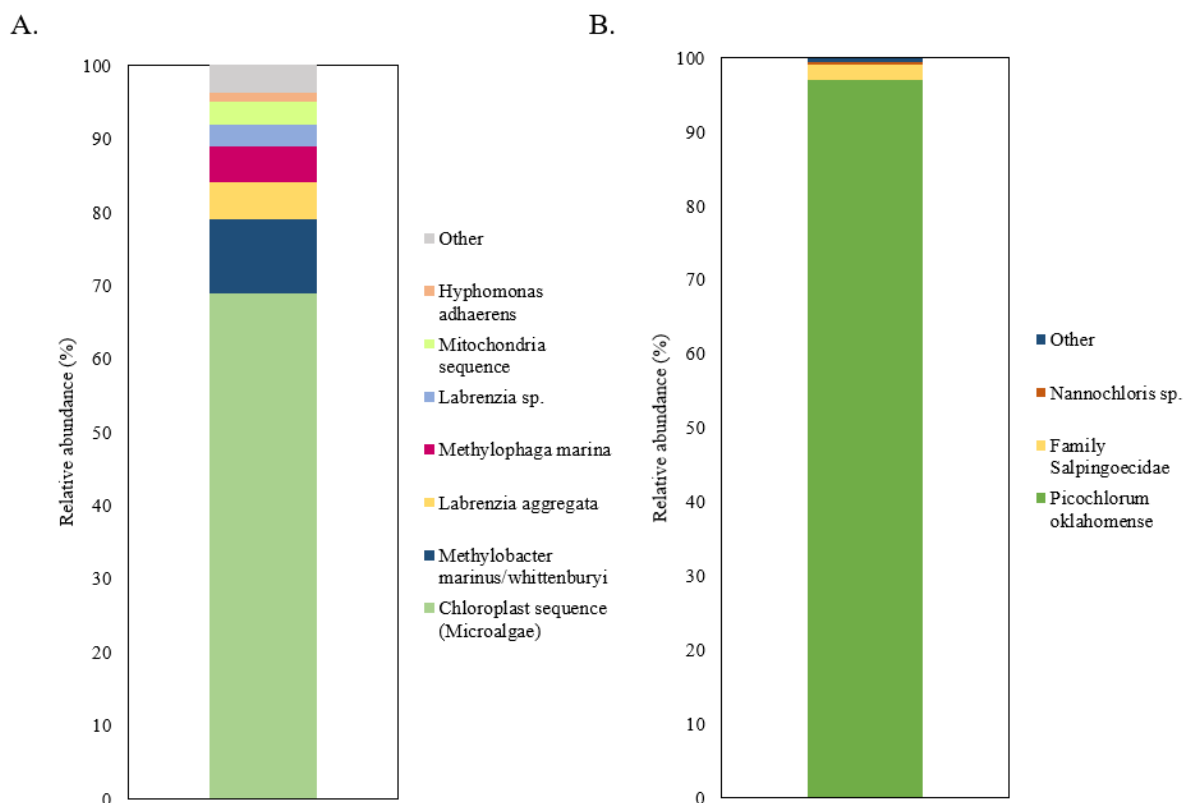


**Figure 12.** Relative abundance of the prokaryotic and eukaryotic amplicon sequencing variants (ASV) found in the Sediment enrichment. A) Prokaryotes. B) Eukaryotes.

**Table 7.** Main characteristics of prokaryotic and eukaryotic organisms related to the sequences retrieved from Sediment enriched sample.

Prokaryotes	Eukaryotes
<p><i>Methylobacter marinus/whittenburyi</i></p> <ul style="list-style-type: none"> <li>- Halophilic Type I methanotroph (pMMO) (Bowman, 2006; Kalyuzhnaya et al., 2008)</li> <li>- Cell size: 0.8 - 2 micrometers (<math>\mu\text{m}</math>) (Orata et al., 2018)</li> <li>- Requires 2% NaCl for growth (Bowman, 2006)</li> <li>- Utilizes methane and methanol as soles sources of carbon and energy (Bowman et al., 1993)</li> </ul>	<p><i>Picochlorum oklahomense</i></p> <ul style="list-style-type: none"> <li>- Chlorophyta microalgae. Conspecific sister species to <i>Nannochloris</i> sp. (Henley et al., 2004)</li> <li>- Small size: 1 to 4 <math>\mu\text{m}</math> (Zhu &amp; Dunford, 2013)</li> <li>- Wide salinity range tolerance: 0-14%. Growth rates decrease with increasing salinity but most stressful conditions for its growth are salinities lower than 2%. (Henley et al., 2004; Zhu &amp; Dunford, 2013)</li> <li>- Historically used for biomass, pigment and lipid production due to high biomass productivity and high-carotenoid content (Zhu &amp; Dunford, 2013)</li> <li>- Common in hypersaline environments but acclimatized to high fluctuations in salinity concentrations (Annan, 2008)</li> </ul>
<p><i>Methylophaga marina</i></p> <ul style="list-style-type: none"> <li>- Marine obligately methanol-utilizing bacteria (Urakami &amp; Komagata, 1987)</li> <li>- Short rod cells sized 0.2 to 2 <math>\mu\text{m}</math> (Janvier et al., 1985)</li> <li>- Optimum temperature: 30 to 37°C (Janvier et al., 1985)</li> <li>- <math>\text{Na}^+</math> and <math>\text{Mg}^{2+}</math> ions are essential for its growth (Janvier et al., 1985)</li> <li>- Tolerance to NaCl up to 12% (Urakami &amp; Komagata, 1987)</li> </ul>	

<p><i>Hyphomonas adhaerens</i></p> <ul style="list-style-type: none"> <li>- Hydrocarbon-degrading bacteria (Atakpa et al., 2023)</li> <li>- Growth in saline environments from 1.5 to 12% NaCl (Weiner et al., 2000)</li> </ul>	<p><i>Nannochloris</i> spp.</p> <ul style="list-style-type: none"> <li>- Marine chlorophytic photosynthetic organism (Chua &amp; Schenk, 2017)</li> <li>- Very adaptable to diverse salinities (from 5 to 35%). However, increasing salinities hinder cell growth (Fakhri et al., 2016)</li> <li>- Historically used for unsaturated fatty acids production for aquaculture due to intrinsic high lipidic content (Fawley et al., 2015)</li> </ul>
<p><i>Labrenzia</i> spp.</p> <ul style="list-style-type: none"> <li>- Heterotrophic and facultatively anaerobic bacteria</li> <li>- Ubiquitous in marine environments with high relevance in N and sulphur cycles. (Zhong et al., 2021)</li> </ul>	<p><i>Hyphomonas adhaerens</i></p> <ul style="list-style-type: none"> <li>- Marine bacteria</li> <li>- Critical link in microbial food chain by nutrient cycling (King, 2005)</li> </ul>

The presence of *Picochlorum oklahomense* in the culture was also confirmed with optical microscopy, as shown in figure 13. The microalgae cells exhibit a coccoid and oblong shape, along with a single chloroplast, consistent with the morphological characteristics of this species (Belkinova et al., 2021). Additionally, various types of bacteria were observed in the culture, but they could not be identified further though microscopic examination alone.

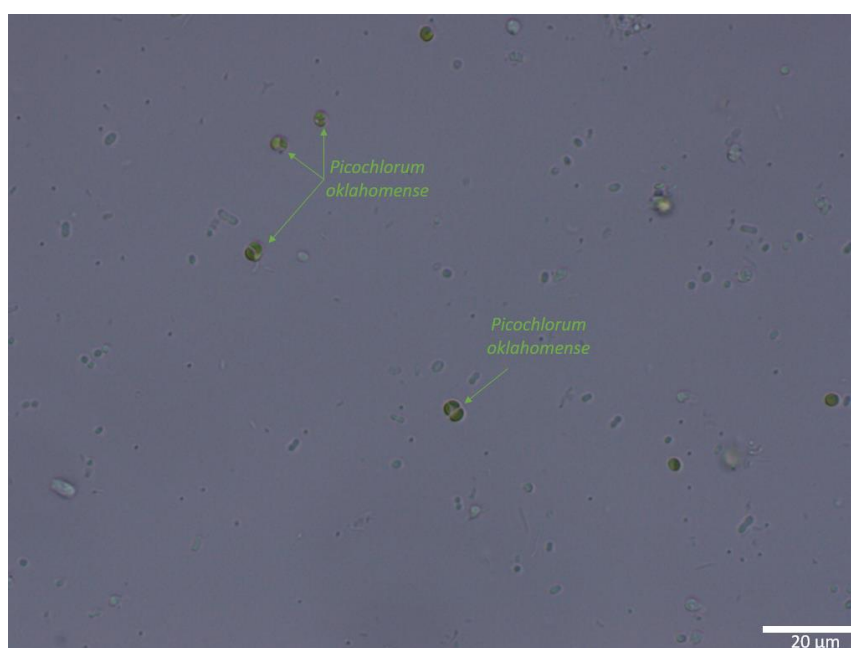


**Figure 13.** Light microscopy image (20x) of the Sediment enrichment showcasing a mixed culture of *Picochlorum oklahomense* and different bacteria.

#### 4.1.4. Ectoine content and biomass growth

A preliminary screening of the ectoine content in the Sediment enrichment was conducted using six randomly selected samples. The aim was to evaluate the enrichment's ability to synthesise, accumulate, and excrete ectoine. Both the supernatant and the biomass were analysed using HPLC-UV (following the procedure outlined in Section 3.5.4) to determine their extracellular and intracellular ectoine content, respectively. The results showed an intracellular ectoine content of  $6.7 \pm 1.4 \text{ mg}_{\text{ectoine}} \text{ g}_{\text{VSS}}^{-1}$ , with no

extracellular ectoine detected at any point. These findings led to the conclusion that the Sediment enrichment was the most suitable for further experiments, based on its optimal CH<sub>4</sub> removal efficiency, the presence and favourable concentration of ectoine in its biomass, and its robust biomass concentration ( $0.94 \pm 0.02 \text{ gVSS L}_{\text{culture}}^{-1}$ ).

## 4.2. Salinity tests: Influence of NaCl concentration on growth, ectoine production and gas consumption

### 4.2.1. Methane removal efficiency and gas concentration in the headspace

After a 14-day incubation period, tests with 0% and 3% NaCl showed significantly higher CH<sub>4</sub> removal efficiencies compared to the 6% and 9% NaCl groups (Kruskal-Wallis test,  $p < 0.0001$ ) (Figure 14). Co-cultures without salinity achieved the highest CH<sub>4</sub> removal efficiency ( $100 \pm 0\%$ ), followed by those at a 3% NaCl concentration ( $92.1 \pm 17.6\%$ ). The CH<sub>4</sub> removal was also associated with increased production and consumption of O<sub>2</sub> and CO<sub>2</sub>, attributed to high microalgal activity (Figure 15). In one of the biological duplicates at 3% and 9% NaCl concentrations, photoinhibition of the microalgae was observed on the fourth day of the experiment (Figure 16). This was caused by excessive light exposure due to the placement of the cultures in a shaker with excess light from a nearby experiment. The increased light intensity led to photoinhibition, reducing the relative abundance of microalgae in these two reactors. This photoinhibition did affect the gas composition in the headspace. In the experimental groups where one duplicate was photoinhibited, the overall O<sub>2</sub> and CO<sub>2</sub> concentrations in the headspace showed a different trend compared to the non-photoinhibited ones due to a lower photosynthetic activity. The reduction in photosynthetic organisms resulted in slightly decreased CO<sub>2</sub> consumption and O<sub>2</sub> production, as illustrated in figure 15. Although there was no complete depletion of O<sub>2</sub> in any case, its abundance in the headspace was lower in the photoinhibited reactor compared to the non-photoinhibited ones, as shown in 3% A and B, and 9% A and B. Specifically, in the biological duplicate 9% B, the lack of CH<sub>4</sub> oxidation allows us to see how more O<sub>2</sub> and less CO<sub>2</sub> can be found in the headspace than the initially present when performing the replenishment due to photosynthetic activity. This does not occur when there is a lower relative abundance of microalgae in the sample. However, this photoinhibition had no significant impact on the CH<sub>4</sub> oxidation capacity of the experiments for both 3% NaCl (Mann-Whitney U test,  $p = 0.2105$ ) and 9% NaCl (t-test,  $p = 0.1793$ ) during the two-day headspace replenishment.

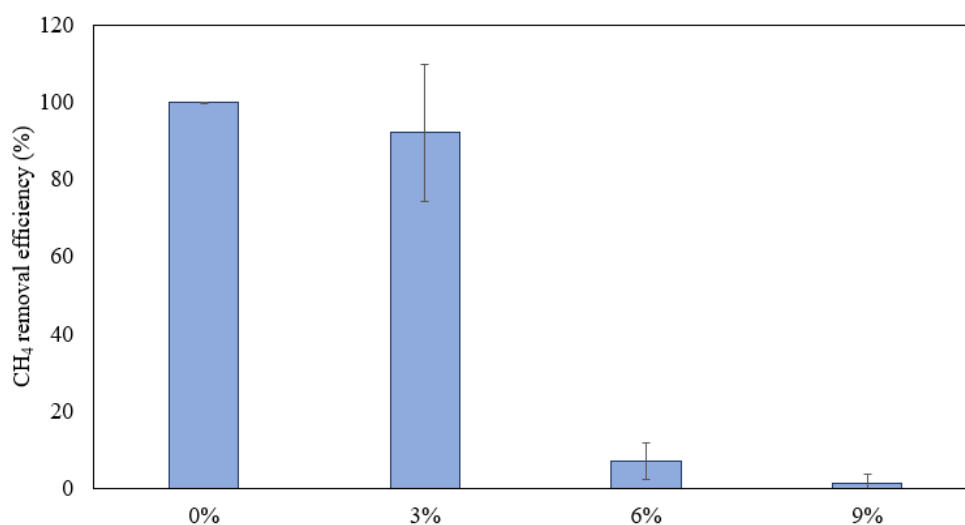


**Figure 14.** Average CH<sub>4</sub> removal efficiency per 2-day replenishment for each NaCl concentration test (0%, 3%, 6% and 9% NaCl). The error bars indicate the standard deviation of biological duplicates.

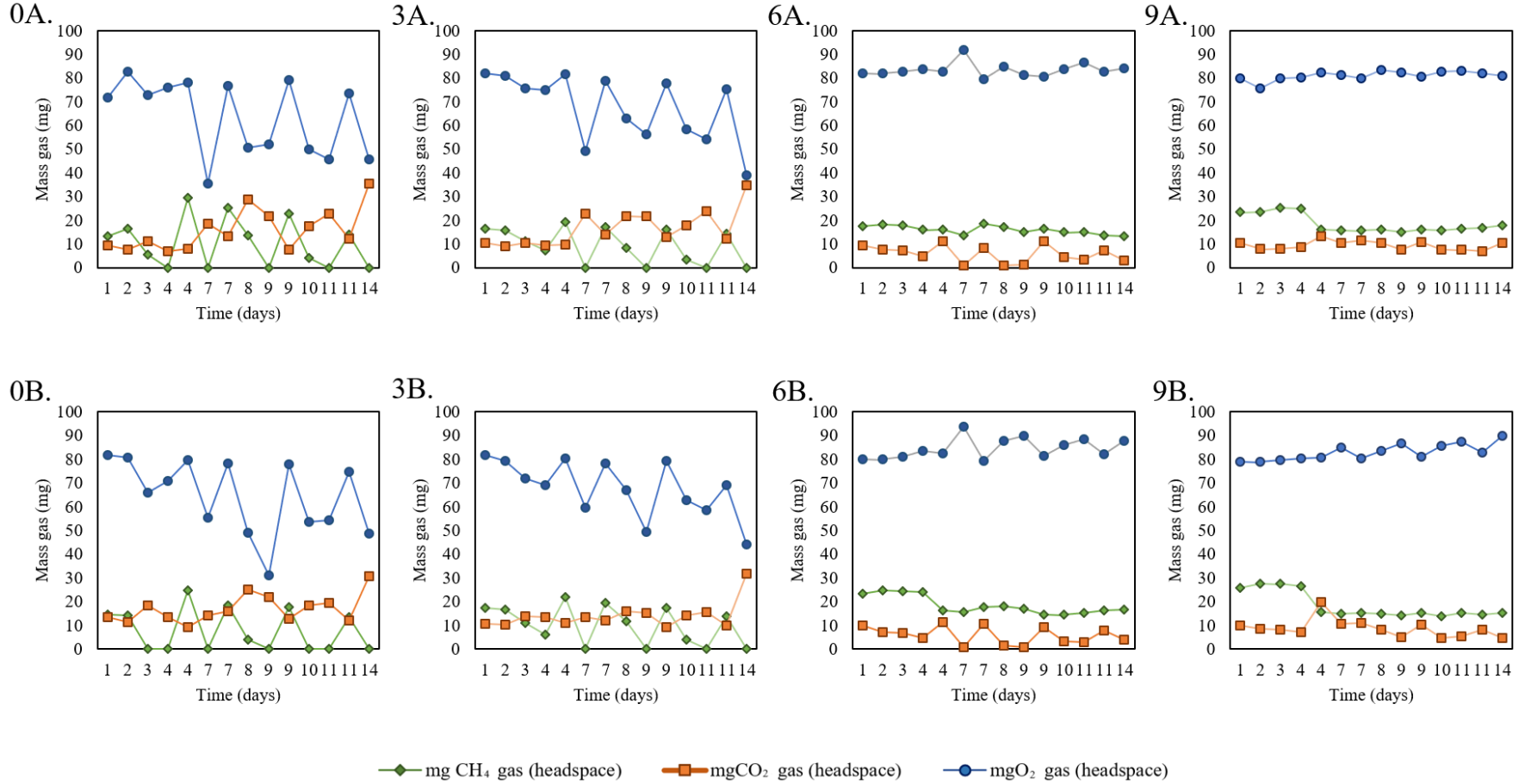


**Figure 15.** Amount of methane (CH<sub>4</sub>), oxygen (O<sub>2</sub>) and carbon dioxide (CO<sub>2</sub>) in milligrams (mg) in the headspace of the experimental groups 0%, 3%, 6% and 9% NaCl during the 14-day experimental period, with headspace replenishment every 2 days, shown as follows: 0A) 0% NaCl biological duplicate 0B) 0% NaCl biological duplicate B. 3A) 3% NaCl biological duplicate A that suffered photoinhibition in the fourth day of incubation 3B) 3% NaCl biological duplicate B. 6A) 6% NaCl biological duplicate 6B) 6% NaCl biological duplicate B. 9A) 9% NaCl biological duplicate A that suffered photoinhibition in the fourth day of incubation. 9B) 9% NaCl biological duplicate B.

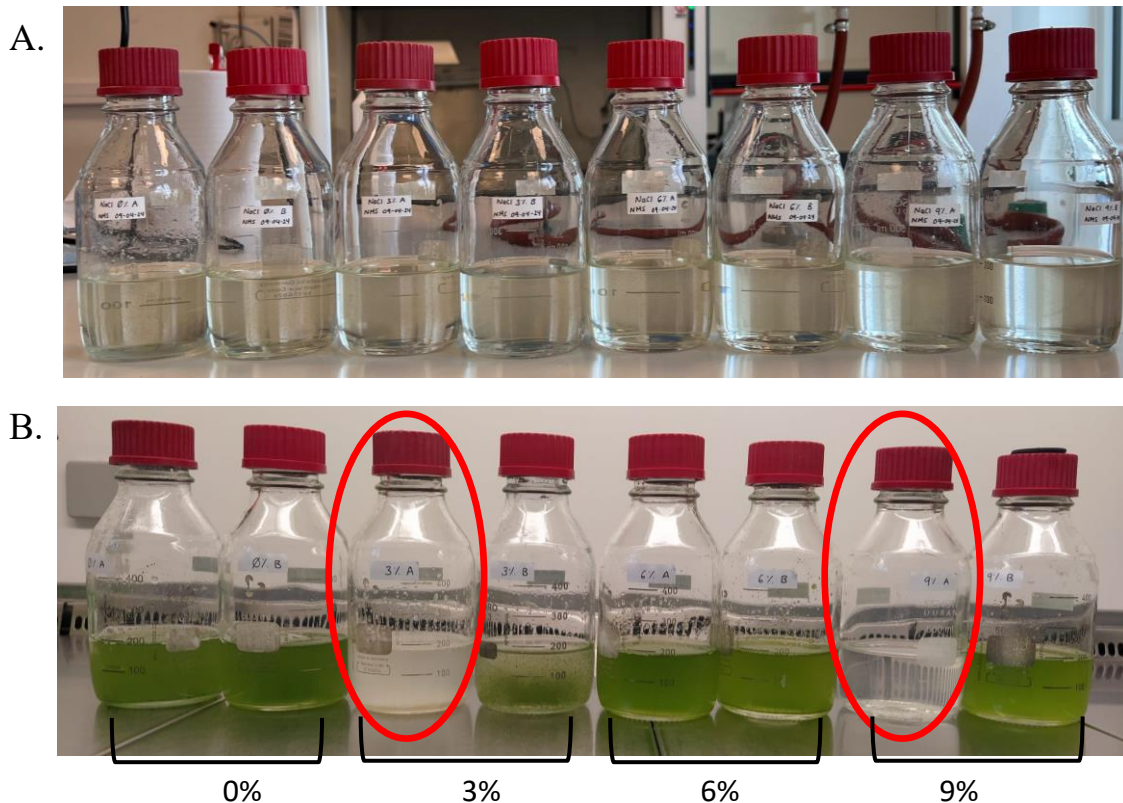


**Figure 16.** Salinity test biological duplicates for NaCl concentrations of 0%, 3%, 6% and 9% at two points: A) start of the experiment and B) after 14-day incubation period. Photoinhibition clearly visible in duplicates 3A and 9A from fourth day onwards and upon completion of the experiment.

#### 4.2.2. Biomass growth and composition

A 17.5-fold increase in biomass ( $g_{VSS}$ ) was observed across all experimental tests after the 14-day incubation period, with an average biomass concentration of  $0.68 \pm 0.03 g_{VSS} L_{culture}^{-1}$  (Figure 17). However, the microbial composition varied significantly between bioreactors, as measured by flow cytometry (FCM) (Figure 18). The experiments that experienced photoinhibition (3% NaCl A and 9% NaCl A) had a microalgae composition of 11% or less, whereas the remaining experiments showed microalgae compositions ranging from 40% to 70%. The rest of the co-culture's relative composition consisted of heterotrophic and methanotrophic bacteria (Figure 18). Cell counting and differentiation were performed by first analysing the filtered medium without any microorganisms using FCM, establishing this as the background noise, and then analysing the size and shape of the microorganisms to perform gating and cell counting of the samples. The photoinhibited experiments further assisted in refining the gating process, as shown in Figure 19.



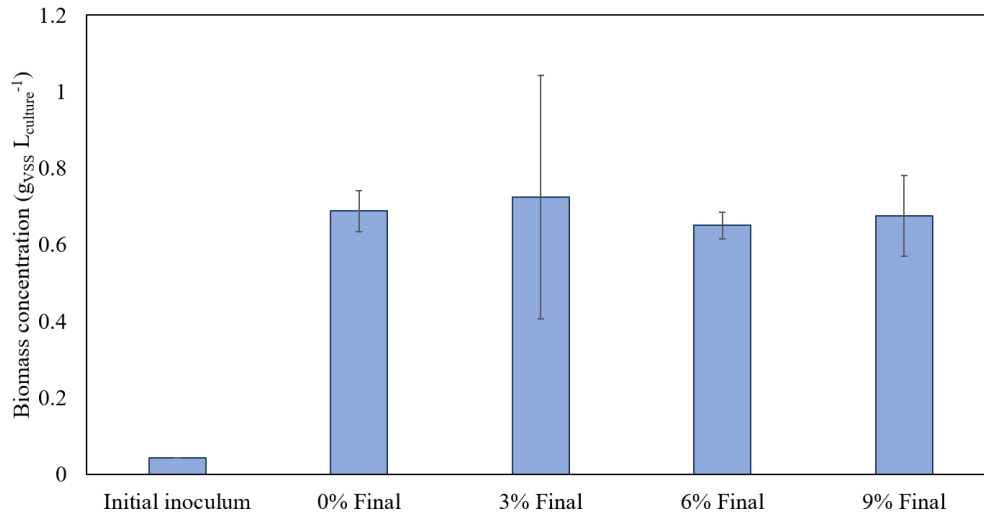


**Figure 17.** Average biomass concentration in g<sub>VSS</sub> L<sub>culture</sub><sup>-1</sup> of the initial inoculum and final measurement of biological duplicates for each salinity concentration test (0%, 3%, 6% and 9%). The error bars indicate the standard deviation of test.

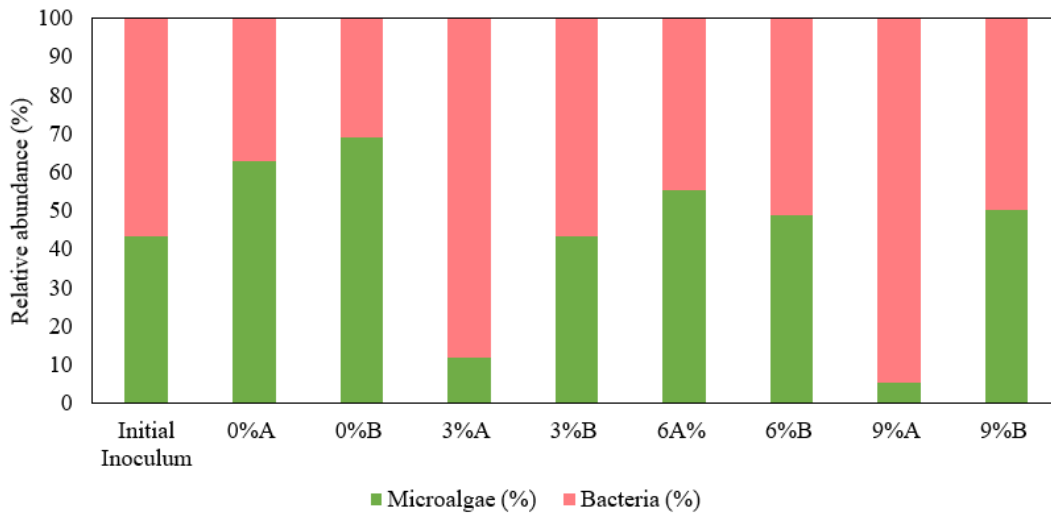


**Figure 18.** Relative abundance (in percentage) of microalgae and heterotrophic/methanotrophic bacteria in the initial inoculum and each salinity test (for both biological duplicates A and B) after 14 days of culture.

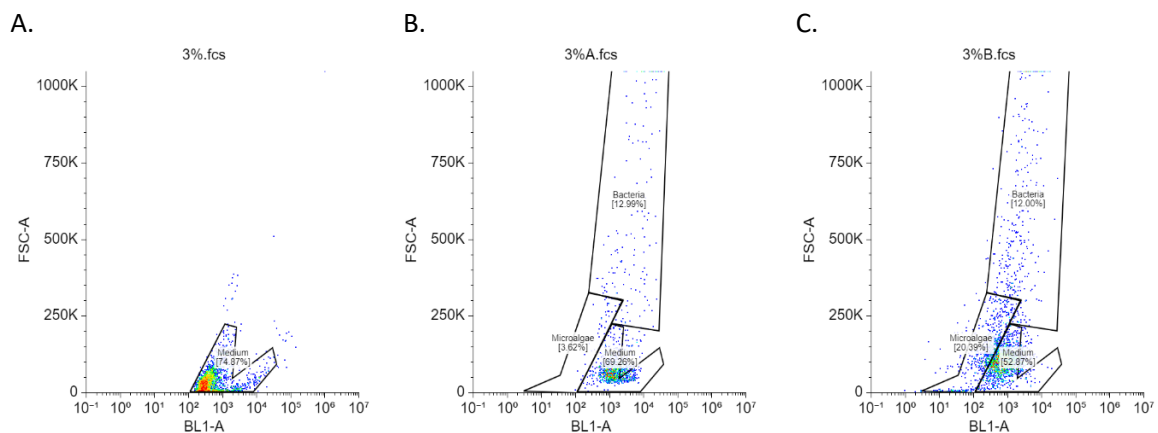


**Figure 19.** Example of FCM results obtained from the 3% experiment, along with the gating performed for microalgae-bacteria determination. A). Filtered mineral salt medium with 3% NaCl. B) 3%A photoinhibited bioreactor. C) 3%B non-photoinhibited bioreactor.

### 4.2.3. Ectoine production

The initial inoculum contained an intracellular ectoine concentration of  $8.6 \pm 0.1 \text{ mg}_{\text{ectoine}} \text{ g}_{\text{VSS}}^{-1}$ . After the 14-day incubation period, the group incubated with 3% NaCl concentration showed a slight increase to  $12.0 \pm 2.7 \text{ mg}_{\text{ectoine}} \text{ g}_{\text{VSS}}^{-1}$ . No ectoine was detected in the biomass of the experimental groups with 0%, 6%, and 9% NaCl concentrations (Figure 20). As observed in the ectoine content measurements of the Sediment enrichments (refer to Section 4.1.4), no extracellular ectoine was detected in the supernatant, indicating that ectoine was not released into the culture media in any of the experiments.

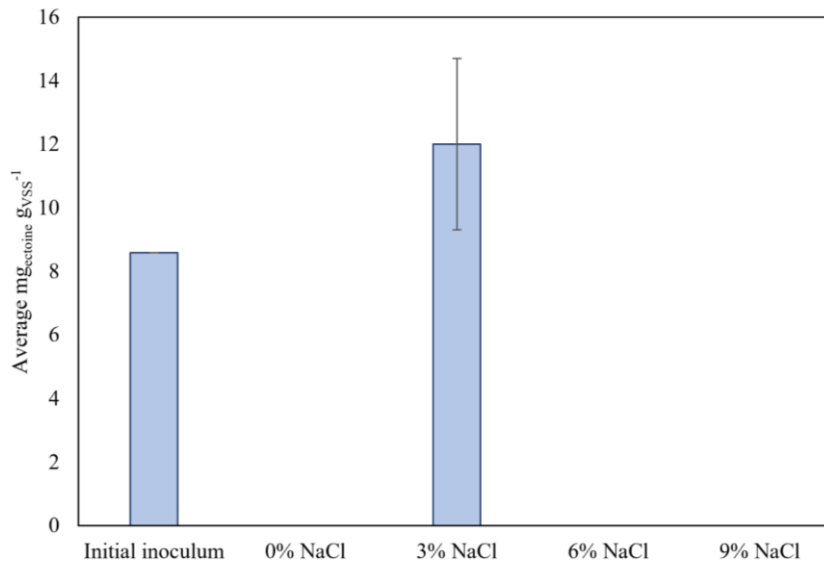


**Figure 20.** Average intracellular ectoine concentration in  $\text{mg}_{\text{ectoine}} \text{ g}_{\text{VSS}}^{-1}$  initially (initial inoculum) and after 14 days of incubation for both biological duplicates at 0%, 3%, 6% and 9% NaCl. The error bars indicate the standard deviation of biological duplicates.

## 4.3. Osmotic shock tests

### 4.3.1. Methane removal efficiency and gas concentrations in the headspace

The impact of varying NaCl concentrations following each osmotic shock was evaluated by analysing the  $\text{CH}_4$  removal efficiency after each experiment replenishment, as illustrated in figure 21. Initially, all samples were grown in a 3% NaCl medium for 7 days, achieving an average  $\text{CH}_4$  removal efficiency of  $52.3 \pm 3.2\%$  on the final day before the experiments commenced. The first osmotic shock, which involved increasing the NaCl concentration to 4.5% in experimental groups OS1 and OS2, did not significantly affect  $\text{CH}_4$  oxidation efficiencies, which remained comparable to those in the 3% NaCl culture medium. However, raising the salinity to 6% during the first shock in the OS3 experiment led to a marked reduction in  $\text{CH}_4$  removal efficiency, with values approximately six times lower over the 24-hour and 48-hour periods, consistent with findings from previous salinity tests (see section 4.1.2).

A second osmotic shock at 4.5% NaCl in OS2 also indicated a slight decline in  $\text{CH}_4$  removal efficiency, though this was not as pronounced as the decrease observed when the medium salinity was increased to 6% in OS1 during the second shock. The detrimental effects of high salinity concentrations were also reflected in the culture's resilience, which showed slight improvements in removal efficiencies in most cases after a final incubation in 3% NaCl, but these improvements were not comparable to the efficiencies observed at the beginning of the experiment.

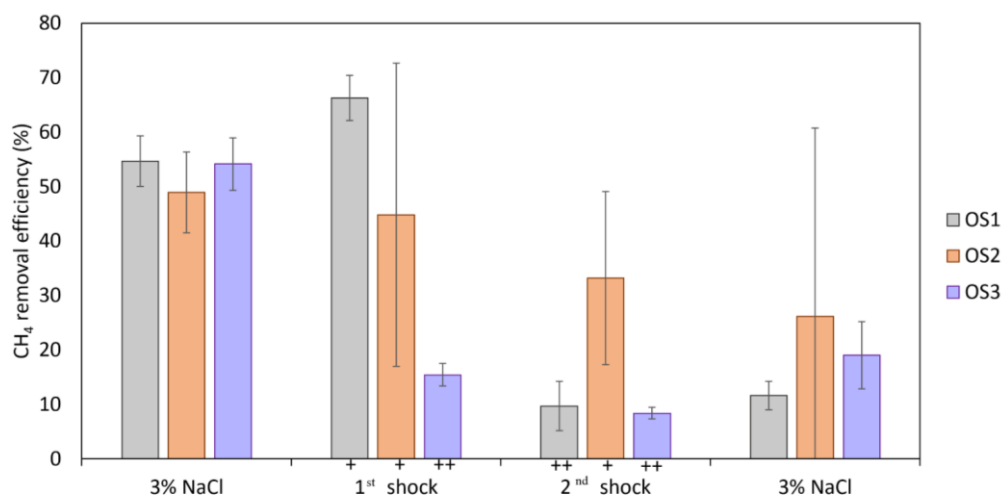


**Figure 21.** Average CH<sub>4</sub> removal efficiencies (and standard deviation in the form of error bars) from biological duplicates with different NaCl concentrations in each replenishment and denoted as OS1, OS2 and OS3 per 1-day replenishment. +: Mineral salt medium with 4.5% NaCl osmotic shock. ++: Mineral salt medium with 6% NaCl osmotic shock. The error bars indicate the standard deviation of each value.

Upon examining the equilibrium dynamics among all gases in the headspace, as illustrated in figure 22, osmotic shocks with 6% NaCl concentration (OS3 in both shocks and OS1 in the second shock) led to a decrease in CH<sub>4</sub> oxidation within the reactors, resulting in reduced O<sub>2</sub> consumption and CO<sub>2</sub> production by methanotrophs. In this case, photosynthetic activity by the microalgae could not be determined as O<sub>2</sub> and CO<sub>2</sub> level fluctuations, despite the reduced CH<sub>4</sub> oxidation, could be likely due to the activity of heterotrophic bacteria. Both OS1 and OS2 exhibited stable activities under a 4.5% NaCl osmotic shocks, while there was a large reduction at 6% NaCl (in the second osmotic shock of the biological duplicates OS1). Here, O<sub>2</sub>, CO<sub>2</sub>, and CH<sub>4</sub> levels remained almost constant, displaying a similar pattern to that observed in OS3 during both shocks.

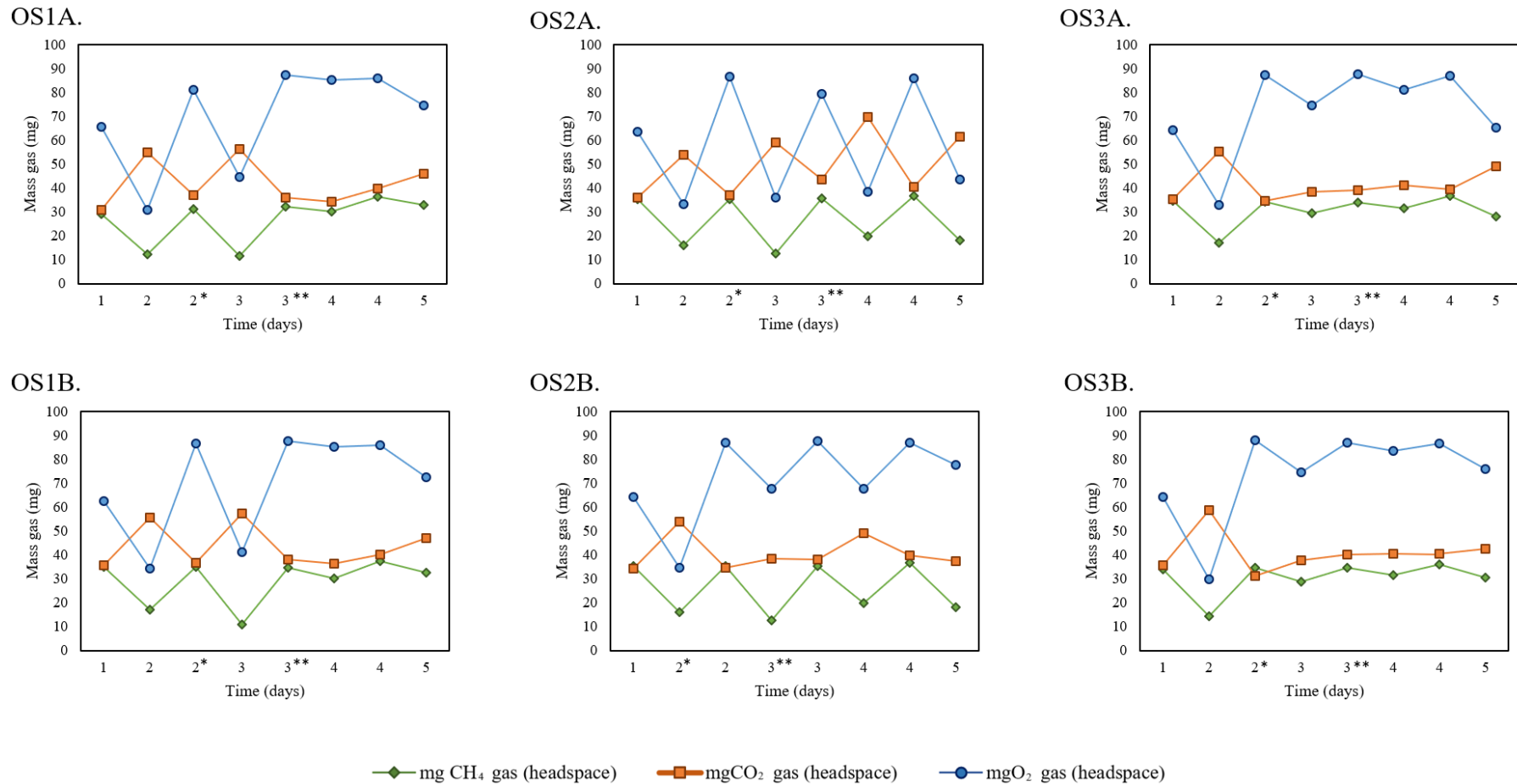


**Figure 22.** Amount of methane (CH<sub>4</sub>), oxygen (O<sub>2</sub>) and carbon dioxide (CO<sub>2</sub>) in milligrams (mg) in the headspace of the experimental groups OS1, OS2 and OS3 during the 5-day osmotic shock tests shown as follows: OS1A. Osmotic shock tests biological duplicate A with first shock (\*) at 4.5% NaCl concentration and second shock at 6% NaCl concentration (\*\*). OS1B. Osmotic shock tests biological duplicate B with first shock (\*) at 4.5% NaCl concentration and second shock at 6% NaCl concentration (\*\*). OS2A. Osmotic shock tests biological duplicate A with first (\*) and second shock (\*\*) at 4.5% NaCl concentration. OS2B. Osmotic shock tests biological duplicate B with first (\*) and second shock (\*\*) at 4.5% NaCl concentration. OS3A. Osmotic shock tests biological duplicate A with first (\*) and second shock (\*\*) at 6% NaCl concentration. OS3B. Osmotic shock tests biological duplicate B with first (\*) and second shock (\*\*) at 6% NaCl concentration. All cultures were maintained in a 3% NaCl concentration medium during days 1 to 2 and 4 to 5 of the experiment.

### 4.3.2. Biomass growth and composition

The reduction in CH<sub>4</sub> oxidation at 6% NaCl (OS3) was not reflected in biomass growth, which nearly doubled after the first salinity shock, increasing from  $0.35 \pm 0.1 \text{ g}_{\text{VSS}} \text{ L}^{-1}$  initially to  $0.65 \pm 0.1 \text{ g}_{\text{VSS}} \text{ L}^{-1}$  after 24 hours. However, the biomass did not vary significantly after the second shock (Figure 23). In contrast, OS2 biomass remained relatively stable during both 4.5% NaCl osmotic shocks, while OS1 experienced drastic changes, with biomass decreasing by almost half after each osmotic shock. Although this biomass reduction in OS1 was not immediately evident in the CH<sub>4</sub> removal efficiency after the first shock (4.5%), it became clearly noticeable after the second shock (6% NaCl). All three experimental groups experienced a reduction close to double their VSS content after being cultured back at 3% NaCl salinity conditions.

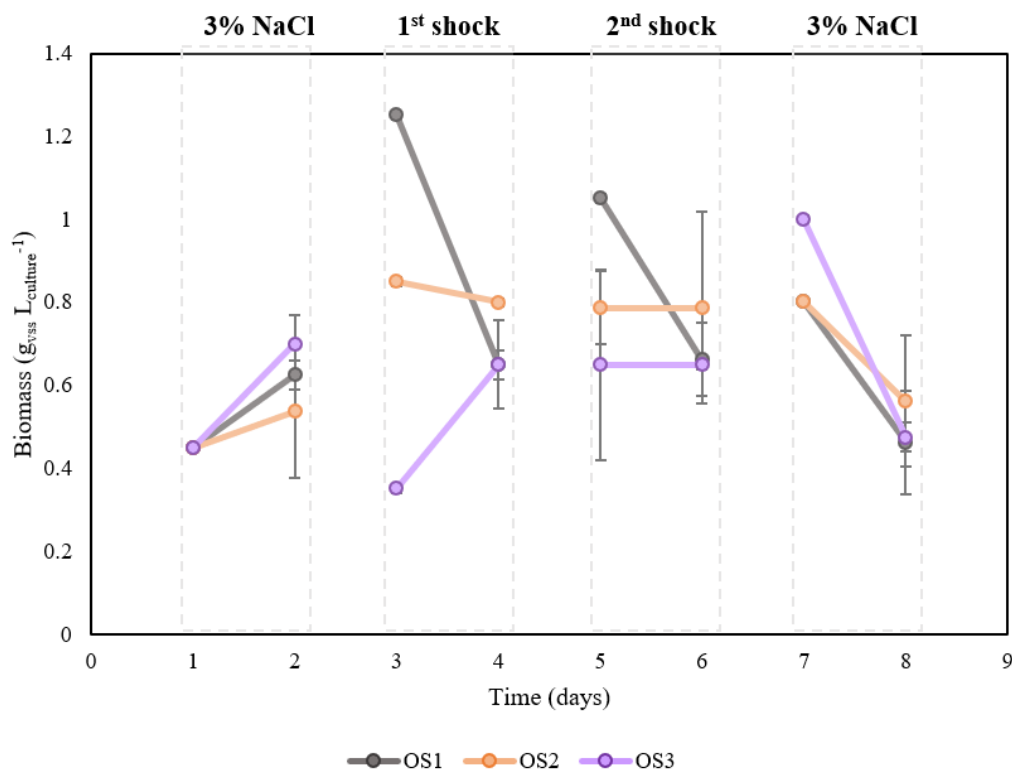


**Figure 23.** Average biomass growth in  $\text{g}_{\text{VSS}} \text{ L}^{-1}$  per 1-day replenishment for the biological duplicates of each osmotic shock test. OS1) initially grown in a mineral salt medium (MSM) containing 3% NaCl followed by a first osmotic shock with raised NaCl concentration (4.5%), a second osmotic shock 6% NaCl content and a final culture back at 3% NaCl content. OS2) initially grown in a MSM containing 3% NaCl followed by a first and second osmotic shocks with raised NaCl concentration (4.5%) and a final culture back at 3% NaCl content. OS3) initially grown in a MSM containing 3% NaCl followed by a first and second osmotic shocks with raised NaCl concentration (6%) and a final culture back at 3% NaCl content. The error bars indicate the standard deviation of each value.

Following the flow cytometry analysis to assess the microbial composition of each experimental group from the osmotic shock experiments, it was found that in both the initial inoculum and the final culture samples, at least 99.9% of the culture consisted of bacteria (including methanotrophic and heterotrophic bacteria), with less than 0.1% comprising microalgae (Appendix 8.2.). Macroscopically, a significant difference was observed between this experiment and the salinity tests, as almost no microalgae were visible in this culture (Figure 24).

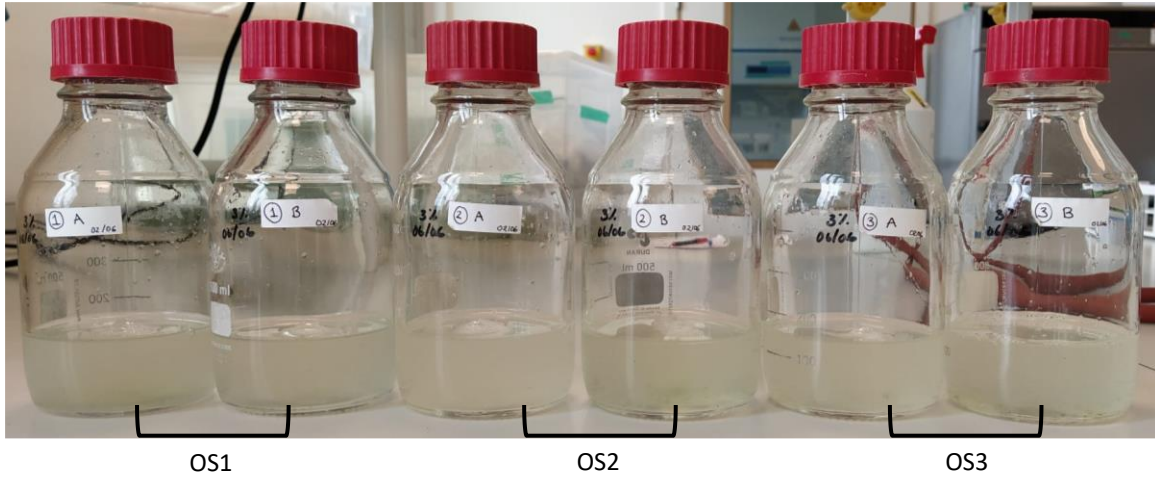


**Figure 24.** Osmotic shock test biological duplicates after 7-day incubation period.

### 4.3.3. Ectoine production

In figure 25, the initial intracellular ectoine concentrations at 3% NaCl were approximately  $31.1 \pm 1.5 \text{ mg}_{\text{ectoine}} \text{ g}_{\text{VSS}}^{-1}$  for all experimental groups. This concentration is higher than the values obtained from ectoine measurements in sediment enrichments (see section 4.1.4) and salinity tests (see section 4.2.3). This increase can be attributed to a greater relative abundance of methanotrophic and heterotrophic bacteria in the co-culture, which accounted for more than 99.9% of the total (Appendix 8.2).

In most instances, final intracellular ectoine concentrations increased after each osmotic shock, reaching a maximum of  $51.3 \pm 1.1 \text{ mg}_{\text{ectoine}} \text{ g}_{\text{VSS}}^{-1}$  for group OS1 following the initial 4.5% NaCl shock (first shock at 24h\*). However, ectoine levels declined (from  $51.3 \pm 1.1 \text{ mg}_{\text{ectoine}} \text{ g}_{\text{VSS}}^{-1}$  to  $42.8 \pm 3.6 \text{ mg}_{\text{ectoine}} \text{ g}_{\text{VSS}}^{-1}$ ) when salinity exceeded 4.5%, as observed at 6% NaCl concentration in group OS1 (second shock at 24h\*\*). This decreased tolerance to higher salinities was also evident in OS3, where final ectoine values were three times lower than those in OS1 and OS2 on both days. Nonetheless, when all cultures were returned to a 3% NaCl medium, ectoine concentrations slightly increased in all cases. Results from OS2 and OS3 also suggest that ectoine levels tend to remain stable during the first 24 and 48 hours if the salinity concentration remains unchanged.

No extracellular ectoine was detected in any of the experimental groups at any point during the experiment. This finding is once again consistent with the results obtained from the Sediment enrichments (see section 4.1.4.) and salinity tests (see section 4.2.3.).

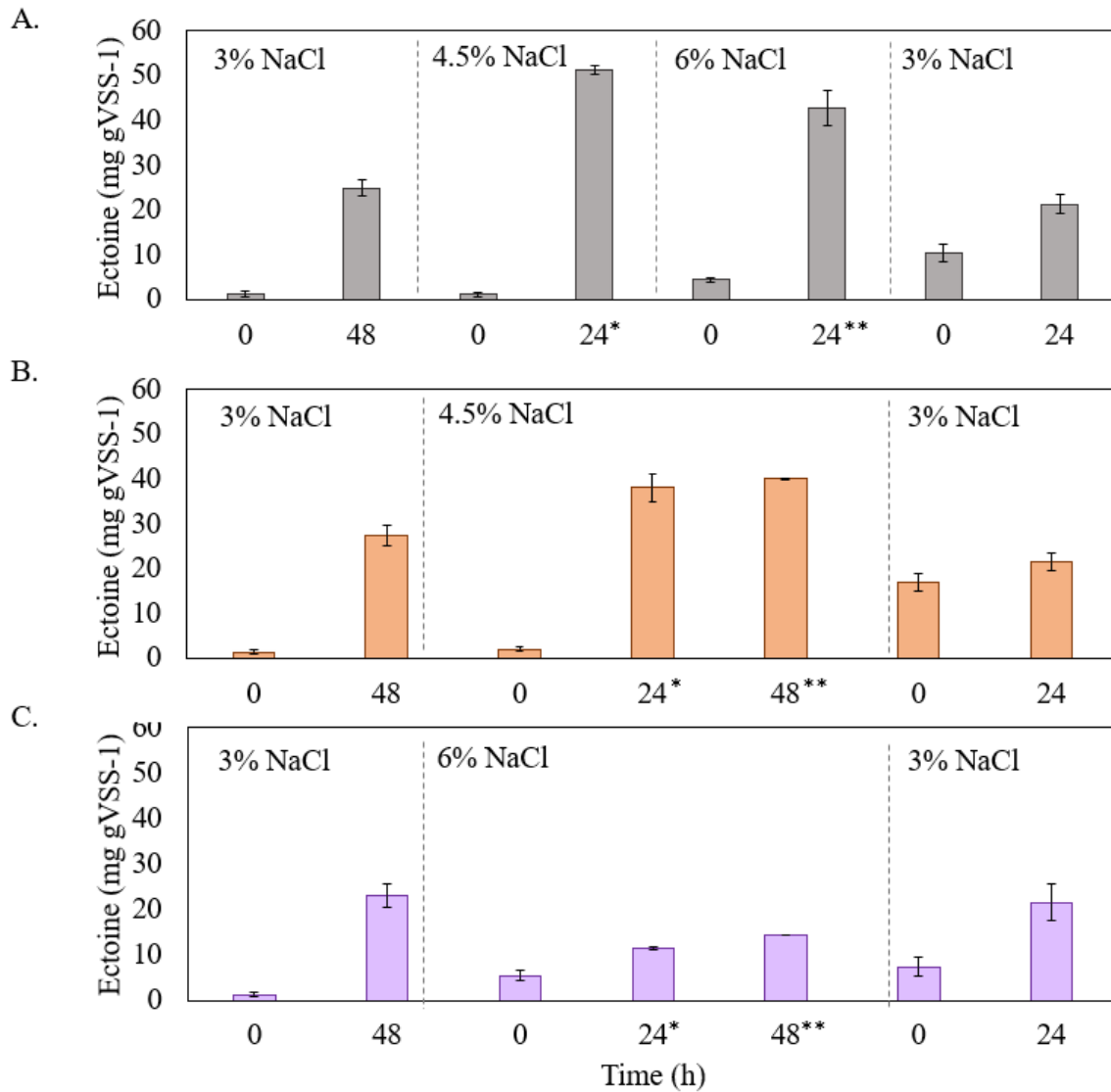


**Figure 25.** Intracellular ectoine concentration measured before the osmotic shock experiments, after first and second shocks, and upon returning to 3% NaCl for the three experimental osmotic shock test groups: OS1, OS2 and OS2. The OS1 experimental group was initially subjected to a 4.5% NaCl shock (first shock: \*) followed by a 6% NaCl osmotic shock (second shock: \*\*). The OS2 group was exposed to a 4.5% NaCl osmotic shock on both days (first and second shock: \* and \*\*), while the OS3 group underwent a 6% NaCl shock on both days (first and second shock: \* and \*\*).

## 5. DISCUSSION

### 5.1. Enrichments from saline environments

The Zwin Natuur park proved to be an appropriate sampling area, as the environmental conditions are ideal for the natural presence of methanotrophic and photosynthetic organisms with halophilic characteristics. Many studies report the presence of methanotrophic bacteria in the North Sea, mainly Type I, with denser populations close to coastal sediments due to the presence of methanogens that produce CH<sub>4</sub> (Vekeman, 2016; Lippmann et al., 2021).

Microalgae constitute the phytoplankton, whose biomass and primary production play a significant role in the marine ecosystem by forming the base of the marine food web, supporting higher trophic levels. Their distribution is spread along shallow and deep areas, with variations in abundance due to geographical, seasonal, and annual factors. However, they dominate the primary production in tidal areas due to the higher light incidence, deposition of organic matter, and more efficient vertical mixing (Reid et al., 1990; Reiss et al., 2006).

Regarding the gas production and consumption rates of each enrichment, marine sediments typically exhibit higher methanotrophic activity than seawater and freshwater for several reasons (Qin et al., 2022; Mao et al., 2022):

- Higher methane availability in the medium because of the decomposition of organic matter by methanogenic archaea, which promotes a higher abundance of methanotrophs.
- Marine sediments provide a more aerobic environment compared to static liquid environments.
- Abundant nutrient and electron acceptor availability, especially in transitional coastal zones.

Sediment environments provide a much more stable nutrient supply compared to seawater and freshwater environments, thus creating a more favourable habitat. Research shows that nutrients like ammonia, nitrate and phosphate are significantly higher in coastal and estuarine sediments than in offshore waters (Zhiliang et al., 1988). This enhanced nutrient richness provides more support to microbial life, resulting in increased methane oxidation and a greater abundance of photosynthetic microorganisms, which in turn leads to more efficient overall methanotrophic activity, as observed in Figure 11.

*Methylobacter marinus/whittenbury* emerged as the main methanotrophic organism in the culture. The presence of this Type I methanotroph is consistent with the growing conditions under which these enrichments were exposed. The MSM medium utilized contains high concentrations of copper (2 mg L<sup>-1</sup> CuSO<sub>4</sub>·5H<sub>2</sub>O) as trace element (Table 4), which plays a crucial role in the methane monooxygenase enzyme (MMO), a copper-dependent enzyme responsible for oxidizing methane to methanol in methanotrophs (see section 1.2.). The MMO enzyme can be particulate (pMMO) or soluble (sMMO). The pMMO is present in most methanotrophs (mainly Type I), with high growing and CH<sub>4</sub> oxidation rates, and expressed when copper is abundant, while sMMO is expressed when copper is limited (Zhu et al., 2022; Murrell et al., 2000; Lee, 2019). As a Type I methanotroph, *Methylobacter marinus/whittenburyi* possesses pMMO, which performs the first step of aerobic methane oxidation. It is a halotolerant species with optimal growth conditions between 0.5 to 2 g NaCl L<sup>-1</sup> (Bowman, 2006) and has been shown to synthesise ectoine as an osmoprotectant in high-salinity environments during methane bioconversion (Sahoo et al., 2021).

*Methylophaga marina* is a halophilic obligate methylotroph which can only grow in one-carbon compounds like methanol, with some strains requiring vitamin B<sub>12</sub> for growth (Janvier et al., 1985). The



presence of this specie in this co-culture can be tightly linked with the methanotrophic activity of *Methylobacter marinus/whittenbury* and the photosynthetic activity of *Picochlorum oklahomense*. The methylotrophs can thrive on the metabolic by-products released by other microorganisms such as methanol, formaldehyde or formate produced by strict methanotrophs or small carbohydrates and aminoacids synthesised during photosynthesis (Dedysh & Dunfield, 2014; Ho et al., 2016).

*Picochlorum oklahomense* is a broadly halotolerant chlorophyte microalgae (Henley et al., 2004) that falls into the “pico” size class of microalgae due to its small size, ranging from 1 to 4 micrometres ( $\mu\text{m}$ ), oblong shape and surrounded by a cell wall (Zhu et al., 2013). This microalga is commonly used for biomass, pigment and lipid production due to its high biomass productivity, rapid growth rates, high-carotenoid content and wide temperature (0 - 40°C), pH and salinity tolerance (0 - 140g L<sup>-1</sup>) (Zhu & Dunford, 2013).

The close interaction of *Methylobacter marinus/whittenbury* with *Picochlorum oklahomense*, forming a synergic community with cross-feeding of metabolites, is essential for its proliferation and can also affect the activity of methylotrophic and non-methanotrophic bacteria (Avila-Nuñez et al., 2024). Hence, even though biogas was used as the sole carbon source, a methylotroph — probably utilized the methanol produced by *Methylobacter marinus/whittenbury* during the CH<sub>4</sub> oxidation process — and diverse non-methanotrophic heterotrophs such as *Hyphomonas adhaerens* and *Labrenzia* sp., were also present in the bioreactor due to it being a natural enrichment. These heterotrophs can use organic substrates (such as methanol, acetate, volatile fatty acids, and polysaccharides) produced by methanotrophs during methane oxidation and microalgae during photosynthesis as metabolic intermediates (Zhang et al., 2023). Some studies also suggest that elevated heterotrophic richness generates complex interactions in co-cultures, potentially stimulating methanotrophic activity, though the specifics are still unclear (Ho et al., 2014). All these factors, as along with the highest CH<sub>4</sub> removal efficiency of all four enrichments, made Sediment the most suitable culture for further experiments.

Regarding the ectoine content, there are studies for both *Methylobacter marinus/whittenbury* and *Methylophaga marina* that show their ability to synthesise and accumulate ectoine. Research indicates that *Methylobacter marinus/whittenbury* can reach ectoine concentrations of up to 5% of dry cell weight for when cultures in 4% NaCl media (Eshinimaev et al., 2007). In contrast, *Methylophaga marina* can accumulate ectoine levels ranging from 15% to 19% of its dry weight in 5% NaCl media (Doronina et al., 2010). These values are significantly higher than the initial ectoine concentrations observed in our enrichment studies, which can be due to the dilution effect caused by microalgae and heterotrophic bacteria in methalgae cultures, as these microorganisms do not synthesise ectoine (Pérez et al., 2022; Ruiz-Ruiz et al., 2020).

## **5.2. Salinity tests: Influence of NaCl concentration on growth, ectoine production and gas consumption**

The NaCl concentrations above 3% negatively impacted CH<sub>4</sub> removal efficiency, with experiments cultured at 0% and 3% NaCl showing 13 times greater CH<sub>4</sub> removal efficiency compared to those at 6% and 9% NaCl, as illustrated in figure 14. This effect may be attributed to the limited halotolerance of methylotrophic bacteria. While these bacteria can grow in saline environments with up to 12% NaCl (Urakami & Komagata, 1987), such conditions are not ideal for their growth. As a result, their growth, abundance, and metabolic activities, including CH<sub>4</sub> oxidation, are hindered (Ho et al., 2018). In contrast, the metabolic activity of microalgae is not affected by varying salinities, as shown in figure 15, where there is even sometimes (for example comparing biological duplicates 9%A and 9%B) net O<sub>2</sub> production compared to the O<sub>2</sub> consumed by bacteria. *Picochlorum oklahomense* is vastly adapted to a wide range of NaCl concentrations, up to 14%. This species is naturally found in hypersaline environments and can withstand significant fluctuations in salinity (Henley et al., 2004; Annan, 2008).

Despite these differences in metabolic activity, the final biomass remains similar across all salinities most likely due to the heterotrophic bacteria, with only minor fluctuations in the relative abundances of each group of microorganisms. Under conditions of no salinity stress or at 3% NaCl, CH<sub>4</sub> removal efficiencies remained consistent with previous experiments. Microalgal activity was unaffected by increased salinity, maintaining similar abundances across all experimental groups except in photoinhibited reactors. The main response of methanotrophs to salinity changes is most evident at zero salinity. In this scenario, the decrease in relative abundance may be due to the methanotrophs' original marine environment, as natural methanotrophic populations from marine settings tend to be less resistant to decreased salinity (Osudar et al., 2017).

Ectoine was detected only in the initial inoculum and the 3% NaCl experimental group, with concentrations ranging from  $8.6 \pm 0.03$  to  $12 \pm 2.70$  mg<sub>ectoine</sub> g<sub>VSS</sub><sup>-1</sup>. The absence of this osmoprotectant molecule at higher salinities, both intracellularly and extracellularly, indicates that no ectoine release into the media occurred. The ectoine present in the initial inoculum may have been degraded, as ectoine synthesis requires significant carbon and nitrogen assimilation, which cannot be sustained when metabolic activity is compromised by high salinity. The degradation of ectoine might affect osmotic balance, but methanotrophs can recycle these valuable nutrients as a last resort for energy (Reshetnikov et al., 2020). Notably, no chlorophyllic microalgae has been confirmed to produce this osmolyte, causing a dilution effect on the culture's ectoine content while also reducing the need for external aeration due to microalgal O<sub>2</sub> production. As noted by Cantera et al. (2016), six percent salinity is not identified as optimal for intracellular ectoine accumulation, with higher concentrations, such as 9%, supporting lower ectoine yields.

### 5.3. Osmotic shock tests

As observed in the salinity test results, a 6% NaCl concentration adversely affected CH<sub>4</sub> removal efficiency, reducing it to levels 4 to 6 times lower than the initial values, depending on whether the starting salinity was 4.5% or 6% NaCl. This negative impact can be due to the limited halotolerance of methylophilic bacteria (Urakami & Komagata, 1987). Additionally, the short intervals at which the osmotic shocks were applied may have influenced the activity of the methanotrophs. Research has indicated that frequent shocks lasting 24 hours or less can induce stress that may either enhance or inhibit CH<sub>4</sub> oxidation, depending on the specific methanotroph species present (Osudar et al., 2017). In this case, the effect would be inhibitory at salinities above 4.5% during the first 24 hours and at salinities greater than 3% after 48 hours or more. This observation aligns with the results obtained in the salinity test experiments (Figure 14). The absence of microalgal species in the culture, as explained in the following paragraph, made it impossible to observe the effects of these osmotic shocks on *Picochlorum oklahomense*.

Concerning the biomass concentration in the culture, the relationship between the osmotic shocks and the biomass concentration does not show a clear pattern. This lack of clarity may be attributed to the significant alterations in the composition of the microbial community within the mixed culture caused by these osmotic shocks. Certain bacterial species may become more dominant, while less adaptable species may experience a decline in abundance after a sudden change in the salinity concentrations of the medium (Bissett et al., 2012). Given the rapid growth rates of these microorganisms, these shifts can occur quite abruptly within just 24 hours following each osmotic shock (Zhu & Dunford, 2013; Kwon et al., 2018). Additionally, methanotrophs typically respond less severely to gradual increases in salinity than to sudden osmotic shocks. Gradual changes provide bacterial cells with more time to adjust their physiological and gene expression responses to the new conditions (Han et al., 2017; Osudar et al., 2017).

In all experimental groups, more than 99% of the biomass was consisted of bacteria (methanotrophic and heterotrophic), with almost no detectable microalgae. This was likely due to the small relative abundance of microalgae in the initial inoculum, which contained only 0.03% microalgae in the culture (Appendix 8.2.). The decrease in microalgae abundance compared to the salinity tests can be attributed to two primary factors: the heterogeneity of the mixed culture, as well as the lower duplication and growth rates of the microalgae relative to the methanotrophs and heterotrophic. The heterogeneity of the mixed culture made it challenging to evenly transfer both bacteria and microalgae to fresh medium. Consequently, a higher percentage of bacteria was introduced during each transfer. Moreover, research indicates that methanotrophic bacteria have growth rates greater than  $0.1 \text{ h}^{-1}$ , with a doubling time of  $18 \text{ h}^{-1}$  (Zhu & Dunford, 2013; Foflonker et al., 2018), while *Picochlorum oklahomense* has a much slower growth rate ranging from  $0.5$  to  $0.9 \text{ day}^{-1}$ , and a doubling time of 1.4 days, depending on salinity as higher salinity levels result in slower growth (Kwon et al., 2018; Amaral & Knowles, 1995). This difference in growth rates and doubling times, along with the importance of the initial biomass ratio, which can affect carbon uptake, methane oxidation efficiencies, and biomass growth (Ruiz-Ruiz et al., 2020), contributed to the dominance of bacteria in the culture.

Ectoine levels reached up to  $51.3 \pm 1.1 \text{ mg}_{\text{ectoine}} \text{ g}_{\text{VSS}}^{-1}$ , consistent with previous studies on the subject (Table 8). These values were higher than those observed in the salinity tests (section 4.2.3) due to a higher abundance of methanotrophic bacteria in the culture (nearly 100%) compared to 30–50% in the salinity tests. Therefore, while microalgae have a dilution effect on the ectoine concentration in the culture, they do enhance the sustainability of the system (Ruiz-Ruiz et al., 2020).

**Table 8.** Specific ectoine values in current methanotroph studies

Microorganism	Ectoine content	Reference
<i>Methylobacterium alcaliphilum</i> 20Z	$66.9 \pm 4.2 \text{ mg}_{\text{ectoine}} \text{ g}_{\text{TSS}}^{-1}$	(Cantera et al. 2016)
<i>Methylobacterium alcaliphilum</i> 20Z	$37.4 \pm 3.8 \text{ mg}_{\text{ectoine}} \text{ g}_{\text{TSS}}^{-1}$	(Cantera et al. 2017)
<i>Methylobacterium alcaliphilum</i> 20Z	$94.2 \pm 10.1 \text{ mg}_{\text{ectoine}} \text{ g}_{\text{TSS}}^{-1}$	(Cantera et al. 2018)
Enrichment of haloalkaliphilic bacteria	$79.7 \pm 5.1 \text{ mg}_{\text{ectoine}} \text{ g}_{\text{TSS}}^{-1}$	
<i>Methylobacterium alcaliphilum</i> 20Z	$20.7 \pm 1.2 \text{ mg}_{\text{ectoine}} \text{ g}_{\text{wet biomass}}^{-1}$	(Mustakhimov et al. 2019)
<i>Methylobacterium alcaliphilum</i> 20Z	$109 \text{ mg}_{\text{ectoine}} \text{ g}_{\text{TSS}}^{-1}$	(Cantera et al. 2020)
Enriched haloalkaliphilic consortium	$3.0 \pm 0.6 \text{ mg}_{\text{ectoine}} \text{ m}^{-3} \text{ h}^{-1}$	
Enriched haloalkaliphilic consortium	$56.6 \pm 2.5 \text{ mg}_{\text{ectoine}} \text{ g}_{\text{VSS}}^{-1}$	(Carmona-Martínez et al. 2021)
<i>Methylobacterium alcaliphilum</i> 20Z	$142.32 \text{ mg}_{\text{ectoine}} \text{ L}^{-1}$	(Cho et al. 2022)
Consortium from salt lagoon	$30 \pm 4 \text{ mg}_{\text{ectoine}} \text{ g}_{\text{VSS}}^{-1}$	(Rodero et al. 2022)
Consortium from salt lagoon	$20\text{-}52 \text{ mg}_{\text{ectoine}} \text{ g}_{\text{VSS}}^{-1}$	(Rodero et al. 2023)

The high heterotrophic and methanotrophic bacterial abundance influenced the overall ectoine content of the biomass in response to the osmotic shocks. Ectoine levels increased with salinities up to 4.5% NaCl, but decreased under more extreme saline conditions (6% NaCl). This reduction in ectoine at high salinities may be due to the physiological stress and potential cellular damage caused by the severe osmotic pressure which can lead to cellular damage or metabolic disruptions. Additionally, the bacteria may start to break down ectoine to use it as a carbon and nitrogen source for metabolism, rather than continuing to accumulate it. This dual role of ectoine—both as an osmoprotectant and a potential energy source—explains the observed decrease in ectoine levels under severe osmotic conditions (Carmona-Martínez et al., 2021; Cantera et al., 2017).

The initial intracellular ectoine concentrations measured during the early stages of the experiments at 3% salinity, as well as after the first osmotic shock, were unexpected. Throughout the course of all experiments, we had not observed any biomass with less than  $6.7 \pm 1.4 \text{ mg}_{\text{ectoine}} \text{ g}_{\text{VSS}}^{-1}$ , whereas in these cases, the values ranged from  $1.91 \pm 0.1 \text{ mg}_{\text{ectoine}} \text{ g}_{\text{VSS}}^{-1}$  to  $4.4 \pm 0.2 \text{ mg}_{\text{ectoine}} \text{ g}_{\text{VSS}}^{-1}$ . These low initial values can be attributed to the centrifugation process during mass sedimentation for medium replenishment, which took approximately three hours. Research has shown that methanotrophic bacteria are adversely affected by mechanical stress. According to Cantera et al. (2016), methanotrophs are particularly sensitive to mechanical agitation, which can impair their ability to produce or maintain ectoine levels. When subjected to this kind of stress, key enzymes encoded in the gene cluster *doeBDAC* are activated allowing methanotrophs to degrade ectoine and integrate it into their metabolism. This mechanism not only helps conserve nitrogen and carbon but also supports energy conservation during stressful conditions. This can be also observed in the significant decrease in ectoine levels following the increase in salinity during the second shock in group OS1, as well as the lack of increase in biomass concentration under sustained stress in groups OS2 and OS3 (Figure 23). This is an environmental adaptation that allows methanotrophs to respond dynamically to changes in their environment, particularly in saline conditions. This adaptability is essential for their survival and efficiency when utilizing methane as their carbon source (Reshetnikov et al., 2020).

For future experiments, the optimal approach would be to isolate the microalgae and methanotrophs species and grow them into separate cultures and then adjust the inoculum ratios to develop the most effective co-culture following a top-down approach. This would allow to tailor the mixed cultures to meet specific requirements for each situation, such as optimizing biomass concentration, maximizing ectoine production, enhancing CH<sub>4</sub> removal and reducing external O<sub>2</sub> supply among others. This would also enable the calculation of the carbon mass balance of the gases in the headspace to evaluate the carbon neutrality of the process.

## 6. CONCLUSIONS AND PERSPECTIVES

Based on the previously discussed results, the following conclusions can be drawn out of this study:

1. **CH<sub>4</sub> oxidation efficiency:** The Sediment enrichment demonstrated the highest average CH<sub>4</sub> oxidation efficiency, reaching 87.7%. In contrast, the Combination enrichment showed lower and more variable CH<sub>4</sub> removal efficiency, while the River and North Sea enrichments exhibited negligible CH<sub>4</sub> removals. This clear difference underlines the importance of selecting suitable environmental settings for microbial cultures aimed at CH<sub>4</sub> removal, as marine sedimentary characteristics promote robust methanotrophic activity.
2. **O<sub>2</sub> and CO<sub>2</sub> dynamics:** Microalgal photosynthetic activity played a crucial role in maintaining a good balance and dynamics between CO<sub>2</sub> and O<sub>2</sub> levels in the headspace. The absence of microalgae in these mixed cultures led to an increase in CO<sub>2</sub> and a reduction in O<sub>2</sub> concentration in the headspace, impacting the methanotrophs' ability to oxidize CH<sub>4</sub> and accumulate ectoine in their biomass.
3. **Dominant species in sediment enrichment:** Microbial composition analysis revealed that *Picochlorum oklahomense*, a microalga extensively adapted to fluctuating salinities and known for its high biomass yields, accounted for 97% of the eukaryotic population. Additionally, the methanotroph *Methylobacter marinus/whittenburyi* and the methylotroph *Methylophaga marina*, represented significant portions of the prokaryotic microbial community. This complex ecosystem, which also includes heterotrophic bacteria, not only facilitated CH<sub>4</sub> oxidation but also created a dynamic system that ensured ecosystem stability and resilience.
4. **Effects of salinity on methane removal and ectoine production:** Salinity tests revealed that higher NaCl concentrations (above 3%) negatively impacted the CH<sub>4</sub> removal efficiencies. The discrepancies in microbial responses under varying salinity levels were evident, with the microalga *Picochlorum oklahomense* maintaining activity despite increased salinity, while methanotrophic bacteria exhibited decreased growth and metabolic rates. Despite limited ectoine production across various salinities, the intracellular content in the initial inoculum and 3% NaCl saline conditions highlighted the innate osmoprotective adaptations of methanotrophs.
5. **Response to osmotic shock:** Osmotic shock experiments indicated that moderate NaCl levels (4.5%) could maintain CH<sub>4</sub> oxidation efficiencies, whereas more extreme conditions led to marked declines in methane oxidation rates. The ectoine levels peaked during 4.5% NaCl osmotic shock conditions. These results suggest that osmoregulatory mechanisms via ectoine synthesis are crucial for microbial adaptability in rapidly fluctuating saline environments.

Future research should focus on unravelling the intricate ecological relationships between microalgae and methanotrophs by isolating each strain and conducting mixed culture experiments using a bottom-up approach. This approach would allow us to delve deeper into the impacts of different stressors, such as temperature, nutrient availability, salinity, and biogas impurities, in a more controlled manner while optimizing conditions for ectoine synthesis. Additionally, research is needed to enhance CO<sub>2</sub> consumption by microalgae, thereby supplying more O<sub>2</sub> to the methanotrophs and ensuring that the process achieves complete carbon neutrality. To transition laboratory findings to real-world applications, pilot-scale experiments should be conducted to evaluate the effectiveness of these enrichments in an industrial setting. However, this presents several operational and biological challenges, such as the complexity of regulating and managing these co-cultures, which can affect operational stability, lead to mass transfer limitations, hinder biomass separation and harvesting, and impact ectoine extraction.

## 7. REFERENCES

- Amaral, J. A., & Knowles, R. (1995). Growth of methanotrophs in methane and oxygen counter gradients. *FEMS Microbiology Letters*, 126(3), 215–220. <https://doi.org/10.1111/j.1574-6968.1995.tb07421.x>
- American Public Health Association. (1998). *Standard methods for the examination of water and wastewater* (20th ed.). Clesceri, L. S., Greenberg, A. E., & Eaton, A. D. (Eds.). American Public Health Association.
- Atakpa, E. O., Yan, B., Okon, S. U., Liu, Q., Zhang, D., & Zhang, C. (2023). Bacterial community response to modified-biochar and exogenous fungi inoculation during degradation of oil-contaminated clayey sediment in slurry phase. *Research Square*. <https://doi.org/10.21203/rs.3.rs-3087242/v1>
- Avila-Nuñez, G., Saldivar, A., Ruiz-Ruiz, P., & Revah, S. (2024). Methanol excretion by *Methylomonas methanica* is induced by the supernatant of a methanotrophic consortium. *Journal of Chemical Technology & Biotechnology*. <https://doi.org/10.1002/jctb.7631>
- Badr, K., Whelan, W., He, Q. P., & Wang, J. (2020). Fast and easy quantitative characterization of methanotroph–photoautotroph cocultures. *Biotechnology and Bioengineering*, 118(2), 703–714. <https://doi.org/10.1002/bit.27603>
- Belkinova, D., Teneva, I., Basheva, D., Neykov, N., Moten, D., Gecheva, G., Apostolova, E., & Naimov, S. (2021). PHYTOPLANKTON COMPOSITION AND ECOLOGICAL TOLERANCE OF THE AUTOTROPHIC PICOPLANKTON IN ATANASOVSKO LAKE (BLACK SEA COASTAL LAGOON, BULGARIA). *Applied Ecology and Environmental Research*, 19(2), 849–866. [https://doi.org/10.15666/aeer/1902\\_849866](https://doi.org/10.15666/aeer/1902_849866)
- Bissett, A., Abell, G. C. J., Bodrossy, L., Richardson, A. E., & Thrall, P. H. (2012). Methanotrophic communities in Australian woodland soils of varying salinity. *FEMS Microbiology Ecology*, 80(3), 685–695. <https://doi.org/10.1111/j.1574-6941.2012.01341.x>
- Bowman, J. (2006). The methanotrophs — the families Methylococcaceae and Methylocystaceae. In *Springer eBooks* (pp. 266–289). [https://doi.org/10.1007/0-387-30745-1\\_15](https://doi.org/10.1007/0-387-30745-1_15)
- Bowman, J. P., Sly, L. I., Nichols, P. D., & Hayward, A. C. (1993). Revised Taxonomy of the Methanotrophs: Description of *Methylobacter* gen. nov., Emendation of *Methylococcus*, Validation of *Methylosinus* and *Methylocystis* Species, and a Proposal that the Family Methylococcaceae Includes Only the Group I Methanotrophs. *International Journal of Systematic Bacteriology*, 43(4), 735–753. <https://doi.org/10.1099/00207713-43-4-735>
- Cantera, S., Lebrero, R., Rodríguez, S., García-Encina, P. A., & Muñoz, R. (2017). Ectoine bio-milking in methanotrophs: A step further towards methane-based bio-refineries into high added-value products. *Chemical Engineering Journal*, 328, 44–48. <https://doi.org/10.1016/j.cej.2017.07.027>
- Cantera, S., Lebrero, R., Sadornil, L., García-Encina, P. A., & Muñoz, R. (2016). Valorization of CH<sub>4</sub> emissions into high-added-value products: Assessing the production of ectoine coupled with CH<sub>4</sub> abatement. *Journal of Environmental Management*, 182, 160–165. <https://doi.org/10.1016/j.jenvman.2016.07.064>
- Cantera, S., Phandanouvong-Lozano, V., Pascual, C., García-Encina, P. A., Lebrero, R., Hay, A., & Muñoz, R. (2020). A systematic comparison of ectoine production from upgraded biogas using *Methylomicrobium alcaliphilum* and a mixed haloalkaliphilic consortium. *Waste Management*, 102, 773–781. <https://doi.org/10.1016/j.wasman.2019.11.043>
- Cantera, S., Sánchez-Andrea, I., Lebrero, R., García-Encina, P., Stams, A. J., & Muñoz, R. (2018). Multi-production of high added market value metabolites from diluted methane emissions via methanotrophic extremophiles. *Bioresource Technology*, 267, 401–407. <https://doi.org/10.1016/j.biortech.2018.07.057>
- Carmona-Martínez, A. A., Marcos-Rodrigo, E., Bordel, S., Marín, D., Herrero-Lobo, R., García-Encina, P. A., & Muñoz, R. (2021). Elucidating the key environmental parameters during the

- production of ectoines from biogas by mixed methanotrophic consortia. *Journal of Environmental Management*, 298, 113462. <https://doi.org/10.1016/j.jenvman.2021.113462>
- Cho, S., Lee, Y. S., Chai, H., Lim, S. E., Na, J. G., & Lee, J. (2022). Enhanced production of ectoine from methane using metabolically engineered *Methylomicrobium alcaliphilum* 20Z. *Biotechnology for Biofuels and Bioproducts*, 15(1). <https://doi.org/10.1186/s13068-022-02104-2>
- Chua, E. T., & Schenk, P. M. (2017). A biorefinery for *Nannochloropsis*: Induction, harvesting, and extraction of EPA-rich oil and high-value protein. *Bioresource Technology*, 244, 1416–1424. <https://doi.org/10.1016/j.biortech.2017.05.124>
- Czech, L., Hermann, L., Stöveken, N., Richter, A. A., Höppner, A., Smits, S. H. J., Heider, J., & Bremer, E. (2018). Role of the extremolytes ectoine and hydroxyectoine as stress protectants and nutrients: genetics, phylogenomics, biochemistry, and structural analysis. *Genes*, 9(4), 177. <https://doi.org/10.3390/genes9040177>
- De Souza, M. F., Meers, E., & Mangini, S. (2024). The potential of microalgae for carbon capture and sequestration. *EFB Bioeconomy Journal*, 4, 100067. <https://doi.org/10.1016/j.bioeco.2024.100067>
- De Vrieze, J. (2020). The next frontier of the anaerobic digestion microbiome: From ecology to process control. *Environmental Science & Ecotechnology*, 3, 100032. <https://doi.org/10.1016/j.esec.2020.100032>
- Dedysh, S. N., & Dunfield, P. F. (2014). Cultivation of methanotrophs. In *Springer protocols handbooks/Springer protocols* (pp. 231–247). [https://doi.org/10.1007/8623\\_2014\\_14](https://doi.org/10.1007/8623_2014_14)
- Doronina, N. V., Ezhov, V. A., Beschastnyi, A. P., & Trotsenko, Y. A. (2010). Biosynthesis of the bioprotectant ectoin by aerobic methylotrophic bacteria from methanol. *Applied Biochemistry and Microbiology*, 46(2), 173–176. <https://doi.org/10.1134/s0003683810020080>
- Eshinimaev, B. T., Tsyrenzhapova, I. S., Khmelenina, V. N., & Trotsenko, Y. A. (2007). Measurement of the content of the osmoprotectant ectoine in methylotrophic bacteria by means of normal-phase high performance liquid chromatography. *Applied Biochemistry and Microbiology*, 43(2), 193–196. <https://doi.org/10.1134/s0003683807020111>
- European Biogas Association. (2021). BIOMETHANE FICHE – Belgium [Report]. <https://energie.wallonie.be/servlet/Repository/biomethane-fiche-be-web.pdf?ID=77201>
- European Commission: Energy, Climate Change, Environment. (2022). *Biomethane*. [https://energy.ec.europa.eu/topics/renewable-energy/bioenergy/biomethane\\_en](https://energy.ec.europa.eu/topics/renewable-energy/bioenergy/biomethane_en)
- European Commission: Energy, Climate Change, Environment. (2023). *Bioenergy Report outlines progress being made across the EU*. [https://energy.ec.europa.eu/news/bioenergy-report-outlines-progress-being-made-across-eu-2023-10-27\\_en](https://energy.ec.europa.eu/news/bioenergy-report-outlines-progress-being-made-across-eu-2023-10-27_en)
- Fakhri, M., Arifin, N. B., Yuniarti, A., & Hariati, A. M. (2016). The Influence of Salinity on the Growth and Chlorophyll Content of *Nannochloropsis* sp. BJ17. *Nature Environment and Pollution Technology*, 16, 2395–3454. [https://neptjournal.com/upload-images/NL-59-30-\(28\)D-517.pdf](https://neptjournal.com/upload-images/NL-59-30-(28)D-517.pdf)
- Fawley, M. W., Jameson, I., & Fawley, K. P. (2015). The phylogeny of the genus *Nannochloropsis* (Monodopsidaceae, Eustigmatophyceae), with descriptions of *N. australis* sp. nov. and *Microchloropsis* gen. nov. *Phycologia*, 54(5), 545–552. <https://doi.org/10.2216/15-60.1>
- Fenizia, S., Thume, K., Wirgenings, M., & Pohnert, G. (2020). Ectoine from Bacterial and Algal Origin Is a Compatible Solute in Microalgae. *Marine Drugs*, 18(1), 42. <https://doi.org/10.3390/md18010042>
- Foflonker, F., Mollegard, D., Ong, M., Yoon, H. S., & Bhattacharya, D. (2018). Genomic analysis of picochlorum species reveals how microalgae may adapt to variable environments. *Molecular Biology and Evolution*. <https://doi.org/10.1093/molbev/msy167>
- Gęsicka, A., Gutowska, N., Palaniappan, S., Oleskiewicz-Popiel, P., & Łężyk, M. (2024). Enrichment of mixed methanotrophic cultures producing polyhydroxyalkanoates (PHAs) from various environmental sources. *Science Of The Total Environment*, 912, 168844. <https://doi.org/10.1016/j.scitotenv.2023.168844>

- Gómez-Borraz, T. L., González-Sánchez, A., Bonilla-Blancas, W., Revah, S., & Noyola, A. (2017). Characterization of the biofiltration of methane emissions from municipal anaerobic effluents. *Process Biochemistry*, 63, 204–213. <https://doi.org/10.1016/j.procbio.2017.08.011>
- González-González, L. M., & De-Bashan, L. E. (2021). Toward the Enhancement of Microalgal Metabolite Production through Microalgae–Bacteria Consortia. *Biology*, 10(4), 282. <https://doi.org/10.3390/biology10040282>
- Han, D., Link, H., & Liesack, W. (2017). Response of *Methylocystis* sp. Strain SC2 to Salt Stress: Physiology, Global Transcriptome, and Amino Acid Profiles. *Applied and Environmental Microbiology*, 83(20). <https://doi.org/10.1128/aem.00866-17>
- Hanson, R. S., & Hanson, T. E. (1996). Methanotrophic bacteria. *Microbiological Reviews*, 60(2), 439–471. <https://doi.org/10.1128/mmr.60.2.439-471.1996>
- Henley, W. J., Hironaka, J. L., Guillou, L., Buchheim, M. A., Buchheim, J. A., Fawley, M. W., & Fawley, K. P. (2004). Phylogenetic analysis of the ‘Nannochloris-like’ algae and diagnoses of *Picochlorum oklahomensis* gen. et sp. nov. (Trebouxiophyceae, Chlorophyta). *Phycologia*, 43(6), 641–652. <https://doi.org/10.2216/i0031-8884-43-6-641.1>
- Hill, E. A., Chrisler, W. B., Beliaev, A. S., & Bernstein, H. C. (2017). A flexible microbial co-culture platform for simultaneous utilization of methane and carbon dioxide from gas feedstocks. *Bioresource Technology*, 228, 250–256. <https://doi.org/10.1016/j.biortech.2016.12.111>
- Ho, A., Angel, R., Veraart, A. J., Daebeler, A., Jia, Z., Kim, S. Y., Kerckhof, F., Boon, N., & Bodelier, P. L. E. (2016). Biotic interactions in microbial communities as modulators of biogeochemical processes: Methanotrophy as a model system. *Frontiers in Microbiology*, 7. <https://doi.org/10.3389/fmicb.2016.01285>
- Ho, A., De Roy, K., Thas, O., De Neve, J., Hoefman, S., Vandamme, P., Heylen, K., & Boon, N. (2014). The more, the merrier: heterotroph richness stimulates methanotrophic activity. *The ISME Journal*, 8(9), 1945–1948. <https://doi.org/10.1038/ismej.2014.74>
- Ho, A., Mo, Y., Lee, H. J., Sauheitl, L., Jia, Z., & Horn, M. A. (2018). Effect of salt stress on aerobic methane oxidation and associated methanotrophs; a microcosm study of a natural community from a non-saline environment. *Soil Biology and Biochemistry*, 125, 210–214. <https://doi.org/10.1016/j.soilbio.2018.07.013>
- IPCC, 2018. Mitigation pathways compatible with 1.5°C in the context of sustainable development. In: Masson-Delmotte, V., et al. (Eds.), *Global Warming of 1.5°C. An IPCC Special Report on the impacts of global warming of 1.5°C above pre-industrial levels and related global greenhouse gas emission pathways, in the context of strengthening the global response to the threat of climate change, sustainable development, and efforts to eradicate poverty*. Intergovernmental Panel on Climate Change, pp. 93–174.
- IPCC, 2023: Sections. In: *Climate Change 2023: Synthesis Report. Contribution of Working Groups I, II and III to the Sixth Assessment Report of the Intergovernmental Panel on Climate Change* [Core Writing Team, H. Lee and J. Romero (eds.)]. IPCC, Geneva, Switzerland, pp. 35-115, doi: 10.59327/IPCC/AR6-9789291691647
- Janvier, M., Frehel, C., Grimont, F., & Gasser, F. (1985). *Methylophaga marina* gen. nov., sp. nov. and *Methylophaga thalassica* sp. nov., Marine Methylophaga. *International Journal of Systematic Bacteriology*, 35(2), 131–139. <https://doi.org/10.1099/00207713-35-2-131>
- Jawaharraj, K., Shrestha, N., Chilkoor, G., Dhiman, S. S., Islam, J., & Gadhamshetty, V. (2020). Valorization of methane from environmental engineering applications: A critical review. *Water Research*, 187, 116400. <https://doi.org/10.1016/j.watres.2020.116400>
- Kalyuzhnaya, M. G., Puri, A. W., & Lidstrom, M. E. (2015). Metabolic engineering in methanotrophic bacteria. *Metabolic Engineering*, 29, 142–152. <https://doi.org/10.1016/j.ymben.2015.03.010>
- Khmelenina, V. N., Murrell, J. C., Smith, T. J., & Trotsenko, Y. A. (2018). Physiology and biochemistry of the aerobic methanotrophs. In *Springer eBooks* (pp. 1–25). [https://doi.org/10.1007/978-3-319-39782-5\\_4-1](https://doi.org/10.1007/978-3-319-39782-5_4-1)
- King, N. (2005). Choanoflagellates. *Current Biology*, 15(4), R113–R114. <https://doi.org/10.1016/j.cub.2005.02.004>



- Klindworth, A., Pruesse, E., Schweer, T., Peplies, J., Quast, C., Horn, M., & Glöckner, F. O. (2012). Evaluation of general 16S ribosomal RNA gene PCR primers for classical and next-generation sequencing-based diversity studies. *Nucleic Acids Research*, 41(1), e1. <https://doi.org/10.1093/nar/gks808>
- Kwon, M., Ho, A., & Yoon, S. (2018). Novel approaches and reasons to isolate methanotrophic bacteria with biotechnological potentials: recent achievements and perspectives. *Applied Microbiology and Biotechnology*, 103(1), 1–8. <https://doi.org/10.1007/s00253-018-9435-1>
- Lee, E. Y. (2019b). Methanotrophs. In *Microbiology monographs*. <https://doi.org/10.1007/978-3-030-23261-0>
- Li, X., Lu, Y., Li, N., Wang, Y., Yu, R., Zhu, G., & Zeng, R. J. (2022). Mixotrophic Cultivation of Microalgae Using Biogas as the Substrate. *Environmental Science & Technology*, 56(6), 3669–3677. <https://doi.org/10.1021/acs.est.1c06831>
- Lim, S. E., Cho, S., Choi, Y., Na, J., & Lee, J. (2024). High production of ectoine from methane in genetically engineered *Methylomicrobium alcaliphilum* 20Z by preventing ectoine degradation. *Microbial Cell Factories*, 23(1). <https://doi.org/10.1186/s12934-024-02404-2>
- Lippmann, T. J. R., Zandt, M. H. I. ', Van Der Putten, N. N. L., Busschers, F. S., Hijma, M. P., Van Der Velden, P., De Groot, T., Van Aalderen, Z., Meisel, O. H., Slomp, C. P., Niemann, H., Jetten, M. S. M., Dolman, H. a. J., & Welte, C. U. (2021). Microbial activity, methane production, and carbon storage in Early Holocene North Sea peats. *Biogeosciences*, 18(19), 5491–5511. <https://doi.org/10.5194/bg-18-5491-2021>
- Liu, M., Liu, H., Shi, M., Jiang, M., Li, L., & Zheng, Y. (2021). Microbial production of ectoine and hydroxyectoine as high-value chemicals. *Microbial Cell Factories*, 20(1). <https://doi.org/10.1186/s12934-021-01567-6>
- Mao, S., Zhang, H., Zhuang, G., Li, X., Liu, Q., Zhou, Z., Wang, W., Li, C., Lu, K., Liu, X., Montgomery, A., Joye, S. B., Zhang, Y., & Yang, G. (2022). Aerobic oxidation of methane significantly reduces global diffusive methane emissions from shallow marine waters. *Nature Communications*, 13(1). <https://doi.org/10.1038/s41467-022-35082-y>
- Marques, A. E., Miranda, J. R., Batista, A. P., & Gouveia, L. (2011). MICROALGAE BIOTECHNOLOGICAL APPLICATIONS: NUTRITION, HEALTH AND ENVIRONMENT. In *Microalgae: Biotechnology, Microbiology and Energy*. Nova Science Publishers.
- Marrazzo, R., & Mazzini, C. (2024). Safety considerations and major accidents prevention in the biogas production. In The Italian Association of Chemical Engineering, *Chemical Engineering Transactions* (Vol. 109, pp. 451–456). AIDIC Servizi S.r.l. <https://www.cetjournal.it/cet/24/109/076.pdf>
- Mekonen, E. A., Mekonnen, Y. T., & Fatoba, S. O. (2023). Thermodynamic prediction of biogas production and combustion: The spontaneity and energy conversion efficiency from photosynthesis to combustion. *Scientific African*, 21, e01776. <https://doi.org/10.1016/j.sciaf.2023.e01776>
- Morais, W. G., Junior, Gorgich, M., Corrêa, P. S., Martins, A. A., Mata, T. M., & Caetano, N. S. (2020). Microalgae for biotechnological applications: Cultivation, harvesting and biomass processing. *Aquaculture*, 528, 735562. <https://doi.org/10.1016/j.aquaculture.2020.735562>
- Murrell, J., McDonald, I. R., & Gilbert, B. (2000). Regulation of expression of methane monooxygenases by copper ions. *Trends in Microbiology*, 8(5), 221–225. [https://doi.org/10.1016/s0966-842x\(00\)01739-x](https://doi.org/10.1016/s0966-842x(00)01739-x)
- Mustakhimov, I. I., Reshetnikov, A. S., But, S. Y., Rozova, O. N., Khmelenina, V. N., & Trotsenko, Y. A. (2019). Engineering of Hydroxyectoine Production based on the *Methylomicrobium alcaliphilum*. *Applied Biochemistry and Microbiology*, 55(6), 626–630. <https://doi.org/10.1134/s0003683819130015>

- Mutanda, T., Naidoo, D., Bwapwa, J. K., & Anandraj, A. (2020). Biotechnological applications of microalgal oleaginous compounds: Current trends on microalgal bioprocessing of products. *Frontiers in Energy Research*, 8. <https://doi.org/10.3389/fenrg.2020.598803>
- Onraedt, A., De Muynck, C., Walcarius, B., Soetaert, W., & Vandamme, E. (2004). Ectoine accumulation in *Brevibacterium epidermis*. *Biotechnology Letters*, 26(19), 1481-1485. <https://doi.org/10.1023/b:bile.0000044448.86907.e4>
- Orata, F. D., Meier-Kolthoff, J. P., Sauvageau, D., & Stein, L. Y. (2018). Phylogenomic analysis of the gammaproteobacterial methanotrophs (Order methylococcales) calls for the reclassification of members at the genus and species levels. *Frontiers in Microbiology*, 9. <https://doi.org/10.3389/fmicb.2018.03162>
- Oren, A., & Garrity, G. M. (2021). Valid publication of the names of forty-two phyla of prokaryotes. *INTERNATIONAL JOURNAL OF SYSTEMATIC AND EVOLUTIONARY MICROBIOLOGY*, 71(10). <https://doi.org/10.1099/ijsem.0.005056>
- Osudar, R., Klings, K., Wagner, D., & Bussmann, I. (2017). Effect of salinity on microbial methane oxidation in freshwater and marine environments. *Aquatic Microbial Ecology*, 80(2), 181–192. <https://doi.org/10.3354/ame01845>
- Pérez, V., Moltó, J. L., Lebrero, R., & Muñoz, R. (2022). Ectoine production from biogas: A sensitivity analysis. Effect of local commodity prices, economy of scale, market trends and biotechnological limitations. *Journal of Cleaner Production*, 369, 133440. <https://doi.org/10.1016/j.jclepro.2022.133440>
- Qin, Q., Kinnaman, F. S., Gosselin, K. M., Liu, N., Treude, T., & Valentine, D. L. (2022). Seasonality of water column methane oxidation and deoxygenation in a dynamic marine environment. *Geochimica Et Cosmochimica Acta*, 336, 219–230. <https://doi.org/10.1016/j.gca.2022.09.017>
- Rasouli, Z., Valverde-Pérez, B., D'Este, M., De Francisci, D., & Angelidaki, I. (2018). Nutrient recovery from industrial wastewater as single cell protein by a co-culture of green microalgae and methanotrophs. *Biochemical Engineering Journal*, 134, 129–135. <https://doi.org/10.1016/j.bej.2018.03.010>
- Reid, P., Lancelot, C., Gieskes, W., Hagmeier, E., & Weichart, G. (1990). Phytoplankton of the North Sea and its dynamics: A review. *Netherlands Journal of Sea Research*, 26(2–4), 295–331. [https://doi.org/10.1016/0077-7579\(90\)90094-w](https://doi.org/10.1016/0077-7579(90)90094-w)
- Reiss, H., Wiekling, G., & Kröncke, I. (2006). Microphytobenthos of the Dogger Bank: a comparison between shallow and deep areas using phytopigment composition of the sediment. *Marine Biology*, 150(6), 1061–1071. <https://doi.org/10.1007/s00227-006-0423-0>
- Reshetnikov, A. S., Rozova, O. N., Trotsenko, Y. A., But, S. Y., Khmelenina, V. N., & Mustakhimov, I. I. (2020). Ectoine degradation pathway in halotolerant methylotrophs. *PLoS ONE*, 15(4), e0232244. <https://doi.org/10.1371/journal.pone.0232244>
- Roberts, N., Hilliard, M., He, Q. P., & Wang, J. (2020). A Microalgae-Methanotroph Coculture is a Promising Platform for Fuels and Chemical Production From Wastewater. *Frontiers in Energy Research*, 8. <https://doi.org/10.3389/fenrg.2020.563352>
- Rodero, M., Carmona-Martínez, A. A., Martínez-Fraile, C., Herrero-Lobo, R., Rodríguez, E., García-Encina, P. A., Peña, M., & Muñoz, R. (2023). Ectoines production from biogas in pilot bubble column bioreactors and their subsequent extraction via bio-milking. *Water Research*, 245, 120665. <https://doi.org/10.1016/j.watres.2023.120665>
- Rodero, M., Herrero-Lobo, R., Pérez, V., & Muñoz, R. (2022). Influence of operational conditions on the performance of biogas bioconversion into ectoines in pilot bubble column bioreactors. *Bioresource Technology*, 358, 127398. <https://doi.org/10.1016/j.biortech.2022.127398>
- Ruiz-Ruiz, P., Estrada, A., & Morales, M. (2020). Carbon dioxide capture and utilization using microalgae. In Elsevier eBooks (pp. 185–206). <https://doi.org/10.1016/b978-0-12-818536-0.00008-7>

- Ruiz-Ruiz, P., Gómez-Borraz, T. L., Revah, S., & Morales, M. (2020). Methanotroph-microalgae co-culture for greenhouse gas mitigation: Effect of initial biomass ratio and methane concentration. *Chemosphere*, 259, 127418. <https://doi.org/10.1016/j.chemosphere.2020.127418>
- Ruiz-Ruiz, P., Gómez-Borraz, T. L., Saldivar, A., Hernández, S., Morales-Ibarria, M., & Revah, S. (2024). Diluted methane mitigation by a co-culture of alkaliphilic methanotrophs and the microalgae *Scenedesmus obtusiusculus* towards carbon neutrality. *Biochemical Engineering Journal*, 203, 109211. <https://doi.org/10.1016/j.bej.2023.109211>
- Safitri, A. S., Hamelin, J., Kommedal, R., & Milferstedt, K. (2021). Engineered methanotrophic syntrophy in photogranule communities removes dissolved methane. *Water Research*, X, 12, 100106. <https://doi.org/10.1016/j.wroa.2021.100106>
- Guerrero-Cruz, S., Vaksmaa, A., Horn, M. A., Niemann, H., Pijuan, M., & Ho, A. (2021). Methanotrophs: discoveries, environmental relevance, and a perspective on current and future applications. *Frontiers in Microbiology*, 12. <https://doi.org/10.3389/fmicb.2021.678057>
- Sahoo, K. K., Goswami, G., & Das, D. (2021). Biotransformation of Methane and Carbon dioxide into High-Value Products by Methanotrophs: Current State of art and Future Prospects. *Frontiers in Microbiology*, 12. <https://doi.org/10.3389/fmicb.2021.636486>
- Salem, R., ElDyasti, A., & Audette, G. F. (2021). Biomedical Applications of Biomolecules Isolated from Methanotrophic Bacteria in Wastewater Treatment Systems. *Biomolecules*, 11(8), 1217. <https://doi.org/10.3390/biom11081217>
- Shedding light on energy in Europe – 2024 edition.* (2024). Eurostat. <https://ec.europa.eu/eurostat/web/interactive-publications/energy-2024>
- Stoeck, T., Bass, D., Nebel, M., Christen, R., Jones, M. D. M., Breiner, H., & Richards, T. A. (2010). Multiple marker parallel tag environmental DNA sequencing reveals a highly complex eukaryotic community in marine anoxic water. *Molecular Ecology*, 19(s1), 21–31. <https://doi.org/10.1111/j.1365-294x.2009.04480.x>
- Strong, P., Kalyuzhnaya, M., Silverman, J., & Clarke, W. (2016). A methanotroph-based biorefinery: Potential scenarios for generating multiple products from a single fermentation. *Bioresource Technology*, 215, 314–323. <https://doi.org/10.1016/j.biortech.2016.04.099>
- Suhartini, S., Lestari, Y. P., & Nurika, I. (2019). Estimation of methane and electricity potential from canteen food waste. *IOP Conference Series Earth and Environmental Science*, 230, 012075. <https://doi.org/10.1088/1755-1315/230/1/012075>
- Tanne, C., Golovina, E. A., Hoekstra, F. A., Meffert, A., & Galinski, E. A. (2014). Glass-forming property of hydroxyectoine is the cause of its superior function as a desiccation protectant. *Frontiers in Microbiology*, 5. <https://doi.org/10.3389/fmicb.2014.00150>
- Urakami, T., & Komagata, K. (1987). Characterization of species of marine methylotrophs of the genus *Methylophaga*. *International Journal of Systematic Bacteriology*, 37(4), 402–406. <https://doi.org/10.1099/00207713-37-4-402>
- Van Der Ha, D., Bundervoet, B., Verstraete, W., & Boon, N. (2011). A sustainable, carbon neutral methane oxidation by a partnership of methane oxidizing communities and microalgae. *Water Research*, 45(9), 2845–2854. <https://doi.org/10.1016/j.watres.2011.03.005>
- Van Der Ha, D., Nachtergaele, L., Kerckhof, F., Rameiyanti, D., Bossier, P., Verstraete, W., & Boon, N. (2012). Conversion of biogas to bioproducts by algae and methane oxidizing bacteria. *Environmental Science & Technology*, 46(24), 13425–13431. <https://doi.org/10.1021/es303929s>
- Vekeman, B. (2016). *Methanotrophic microbiomes from North Sea sediment.* <https://biblio.ugent.be/publication/8075279/file/8075285.pdf>
- Wahyuni, S., Sutjahjo, S. H., Purwanto, Y. A., Fuah, A. M., & Kurniawan, R. (2018). Application of small digester biogas for energy supply in rural areas. *IOP Conference Series Earth and Environmental Science*, 141, 012035. <https://doi.org/10.1088/1755-1315/141/1/012035>
- Wang, D., Zhu, M., Lian, S., Zou, H., Fu, S., & Guo, R. (2022). Conversion of Renewable Biogas into Single-Cell Protein Using a Combined Microalga- and Methane-Oxidizing Bacterial System. *ACS ES&T Engineering*, 2(12), 2317–2325. <https://doi.org/10.1021/acsestengg.2c00237>

- Weiner, R. M., Melick, M., O'Neill, K., & Quintero, E. (2000). *Hyphomonas adhaerens* sp. nov., *Hyphomonas johnsonii* sp. nov. and *Hyphomonas rosenbergii* sp. nov., marine budding and prosthecate bacteria. *INTERNATIONAL JOURNAL OF SYSTEMATIC AND EVOLUTIONARY MICROBIOLOGY*, 50(2), 459–469. <https://doi.org/10.1099/00207713-50-2-459>
- Yang, X., Liu, L., Yin, Z., Wang, X., Wang, S., & Ye, Z. (2020). Quantifying photosynthetic performance of phytoplankton based on photosynthesis–irradiance response models. *Environmental Sciences Europe*, 32(1). <https://doi.org/10.1186/s12302-020-00306-9>
- Yun, J., Lee, H., Nam, J., Ko, M., Park, J., Lee, D., Lee, S., & Kim, H. (2024). Unlocking synergies: Harnessing the potential of biological methane sequestration through metabolic coupling between *Methylomicrobium alcaliphilum* 20Z and *Chlorella* sp. HS2. *Bioresource Technology*, 399, 130607. <https://doi.org/10.1016/j.biortech.2024.130607>
- Zhang, B., Cai, C., & Zhou, Y. (2023). Iron and nitrogen regulate carbon transformation in a methanotroph-microalgae system. *Science of the Total Environment*, 904, 166287. <https://doi.org/10.1016/j.scitotenv.2023.166287>
- Zhang, X. (2018). *Microalgae removal of CO2 from flue gas*. IEA Clean Coal Centre. <https://doi.org/10.13140/RG.2.2.26617.77929>
- Zhiliang, S., Xingjun, L., & Jiaping, L. (1988). Nutrients in seawater and interstitial water of the sediments in the Huanghe River estuarine area (November). *Chinese Journal of Oceanology and Limnology*, 6(2), 104–114. <https://doi.org/10.1007/bf02847830>
- Zhong, H., Sun, H., Liu, R., Zhan, Y., Huang, X., Ju, F., & Zhang, X. (2021). Comparative Genomic Analysis of *Labrenzia aggregata* (Alphaproteobacteria) Strains Isolated From the Mariana Trench: Insights Into the Metabolic Potentials and Biogeochemical Functions. *Frontiers in Microbiology*, 12. <https://doi.org/10.3389/fmicb.2021.770370>
- Zhu, Y., & Dunford, N. T. (2013). Growth and Biomass Characteristics of *Picochlorum oklahomensis* and *Nannochloropsis oculata*. *Journal of the American Oil Chemists Society*, 90(6), 841–849. <https://doi.org/10.1007/s11746-013-2225-0>
- Zhu, Y., Koo, C. W., Cassidy, C. K., Spink, M. C., Ni, T., Zanetti-Domingues, L. C., Bateman, B., Martin-Fernandez, M. L., Shen, J., Sheng, Y., Song, Y., Yang, Z., Rosenzweig, A. C., & Zhang, P. (2022). Structure and activity of particulate methane monooxygenase arrays in methanotrophs. *Nature Communications*, 13(1). <https://doi.org/10.1038/s41467-022-32752-9>

## 8. APPENDIX

### 8.1. Comparative analysis of economic viability of methanotrophic biomass calculations for ectoine production versus biogas combustion for energy production

#### ASSUMPTIONS

For biogas containing 60% CH<sub>4</sub> and 40% CO<sub>2</sub>

0.853	g biomass	-	1	g CH <sub>4</sub>	
0.5118	g biomass	-	1	g biogas	
1	m <sup>3</sup> biogas	-	0.46	kg biogas	(Wahyuni et al., 2018)
70	mg ectoine	-	1	g biomass	(Jawaharraj et al., 2020)
1	mol biogas	-	16.04	g biogas	
0.435	€ / kWh	Electricity price in Belgium 2023 (Eurostat, 2024)			
45%	Electricity generation efficiency (with no heat harnessing)				(Suhartini et al., 2019)
1	m <sup>3</sup> biogas	-	7.861111	kWh	
1	m <sup>3</sup> biogas	-	28.3	MJ	
1	mol biogas	-	534.861	kJ	(Mekonen et al., 2023)
			0.534861	MJ	
Ectoine price	600	€ / kg			
	1000	€ / kg			

#### CALCULATIONS

1	kg biogas	=	62.3441397	mol biogas	
			0.5118	kg biomass	
			511.8	g biomass	
			35826	mg ectoine	
			35.826	g ectoine	
1	mol biogas	=	16.04	g biogas	
			8.209272	g biomass	
			574.64904	mg ectoine / mol biogas	
			0.00057465	kg ectoine / mol biogas	
			0.534861	MJ	
			0.1485725	kWh	
	Electricity		0.064629038	€ / mol biogas	
	Ectoine (Assuming 600 euros/kg ectoine)		0.344789424	€ / mol biogas	
	Ectoine (Assuming 1000 euros/kg ectoine)		0.57464904	€ / mol biogas	
	Ectoine (Assuming 600 euros/kg ectoine)		21.4956	€ / kg biogas	

	Ectoine (Assuming 1000 euros/kg ectoine)		35.826	€ / kg biogas
	Ectoine (Assuming 600 euros/kg ectoine)		9.887976	€ / m <sup>3</sup> biogas
	Ectoine (Assuming 1000 euros/kg ectoine)		16.47996	€ / m <sup>3</sup> biogas
1	m <sup>3</sup> biogas	-	3.419583	€ / m <sup>3</sup> biogas

## 8.2. Shock tests FCM results

**Table 9.** Microbial composition of the shock tests experimental groups OS1, OS2, OS3 obtained from FCM analysis.

	OS1		OS2		OS3	
	Microalgae (%)	Bacteria (%)	Microalgae (%)	Bacteria (%)	Microalgae (%)	Bacteria (%)
<b>Initial inoculum (3% NaCl)</b>	0.03	99.97	0.03	99.97	0.03	99.97
<b>Final 3% NaCl</b>	0.00	100.00	0.00	100.00	0.00	100.00
<b>Initial 1st shock</b>	0.03	99.97	0.01	99.99	0.04	99.96
<b>Final 1st shock</b>	0.00	100.00	0.00	100.00	0.00	100.00
<b>Initial 2nd shock</b>	0.09	99.91	0.00	100.00	0.00	100.00
<b>Final 2nd shock</b>	0.00	100.00	0.00	100.00	0.00	100.00
<b>Initial after shock</b>	0.06	99.94	0.03	99.97	0.06	99.94
<b>Final after shock</b>	0.00	100.00	0.00	100.00	0.00	100.00